NASA Technical Memorandum 78572

Field Measurements of Penetrator Seismic Coupling in Sediments and Volcanic Rocks

Yosio Nakamura, Gary V. Latham, Cliff Frohlich, Maxwell B. Blanchard, and James P. Murphy

April 1979

National Aeronautics and Space Administration

NASA Technical Memorandum 78572

Field Measurements of Penetrator Seismic Coupling in Sediments and Volcanic Rocks

Yosio Nakamura
Gary V. Latham
Cliff Frohlich, The University of Texas, Marine Science Institute
Galveston Geophysics Laboratory, Galveston, Texas
Maxwell B. Blanchard, NASA, Johnson Space Center, Houston, Texas
James P. Murphy, NASA, Ames Research Center, Moffett Field, California

National Aeronautics and
Space Administration

Ames Research Center
Moffett Field, California 94035

FIELD MEASUREMENTS OF PENETRATOR SEISMIC COUPLING IN SEDIMENTS AND VOLCANIC ROCKS

Yosio Nakamura,* Gary V. Latham,* Cliff Frohlich,* Maxwell B. Blanchard† and James P. Murphy‡

I. INTRODUCTION

The use of penetrators for the emplacement of seismic sensors has been given serious consideration in recent years (ref. 1). A network of seismometers deployed on the Martian surface by penetrators is now considered an attractive option for future Mars missions (refs. 2 and 3). Installation of a properly designed seismic network is essential to the achievement of a first-order understanding of the dynamics and internal structure of Mars. In planning to use penetrators for this purpose, it has been assumed that the penetrator body is well coupled to the surrounding medium when emplaced in normal operation. However, excavation of embedded penetrators has revealed that they are usually surrounded by a thin shell of crushed material (refs. 4 and 5). This has raised a question as to whether they may be partially decoupled from the surrounding medium in the frequency band of interest in seismic studies.

As far as we know, theoretical studies on this problem are either lacking or, at best, are insufficient. A study by Woodward-Clyde Consultants (ref. 6) treats the response of a penetrator statically placed in a marine sediment environment, but the effect of the disturbed zone around a dynamically emplaced penetrator is not considered.

A field experiment was planned and executed in order to assess how well penetrators are coupled to the ground. The specific purpose of the experiment was to determine whether there is any significant difference in response, within the frequency band of interest to seismology, between a seismometer mounted on an embedded penetrator, with the impact-crushed zone surrounding it, and a seismometer mounted directly into the undisturbed rocks. In other words, we wished to find out whether a seismometer mounted on an embedded penetrator can function as well as a seismometer statically emplaced by conventional methods. The problem of the movement of a seismometer relative to the true ground motion (absolute response) is a subject in itself, and is not addressed in this study.

The penetrators used in the experiment were exactly one half as large as those designed for use on Mars. Dry-lake bed deposits and volcanic rocks were chosen as targets, representing media of widely differing material properties.

---

*The University of Texas, Marine Science Institute; Galveston Geophysics Laboratory, Galveston, Tex. 77550.
†Johnson Space Center, NASA, Houston, Tex. 77058
‡Ames Research Center, Moffett Field, Calif. 94035

The field measurements were conducted on a dry-lake bed located in the Sandia Test Range near Tonopah, Nevada, on 9-12 October, 1978, and on a basaltic lava flow located in the White Sands Missile Range near Tularosa, New Mexico, on 24-26 October, 1978.

In this report, we describe the experimental setup used for the field measurement, describe the field tests, and present and discuss the results of the analysis performed on the field data. Finally, we present our conclusions and recommendations as to the use of penetrators for seismometer installation.

II. MEASUREMENT SETUP

Figure 1 is a block diagram of the field and laboratory setups for the experiment. Two three-component geophone assemblies were used for detection of seismic signals. One was mounted on the aft end of the penetrator, using an adapter bracket to ensure verticality of the geophone assembly in case the penetrator was embedded at angle. The other, used as a reference, was installed on or in the undisturbed ground using the best methods we could devise to ensure good coupling to the ground. The installation methods will be described in detail later. Mark Products L-10-3D geophone assemblies, each containing a matched set of one vertical- and two horizontal-component geophones with natural frequencies of 4.5 Hz and coil resistances of 940 Ω, were used. The nominal frequency response of the geophones to ground velocity, with a 7.5 kΩ damping resistor to give a damping factor of 0.71, is shown in figure 2. The measured responses are within +0.3 and -0.8 dB of the nominal values for frequencies above 6 Hz, and within +1.2 and -1.0 dB of the nominal values for frequencies below 6 Hz. The geophone assembly is encased in a cylindrical aluminum housing with a diameter of 6.4 cm (2.5 in.) and a total length of 20 cm (7.9 in.). The weight of the assembly is about 1.5 kg.

Signals from each geophone assembly were fed, through a 5-m, six-conductor cable, into a three-channel amplifier set. The amplifiers were designed and built in our laboratory for this experiment. Figure 3 shows the average measured response of the amplifiers at their minimum gain setting. The gain is adjustable between 40 and 70 dB in 6-dB steps. The three response curves (A, B, and C) represent those of (A) the original design used for most of the Tonopah test, (B) extended high frequency (field modified) used in some of the Tonopah test, and (C) the final design used in the White Sands test. Responses of individual amplifiers are matched to within ±0.5 dB.

The amplified signals were transmitted through a pair of 35-m (115 ft) six-conductor cables to a recording setup located inside a van, which was parked about 30 m (100 ft) away from the geophones. Two types of recording devices were used: a Gould Brush 260, six-channel chart recorder for real-time, visible recording; and a Bell and Howell, Astro-Sciences M-14G, six-channel FM (IRIG wide-band gruop 1) instrumentation tape recorder to record data in a form suitable for later laboratory analysis. Owing to an equipment problem, the Bell and Howell recorder was replaced by an Ampex FR-1300 recorder (IRIG intermediate-band FM) for the last few shots of the White Sands test.

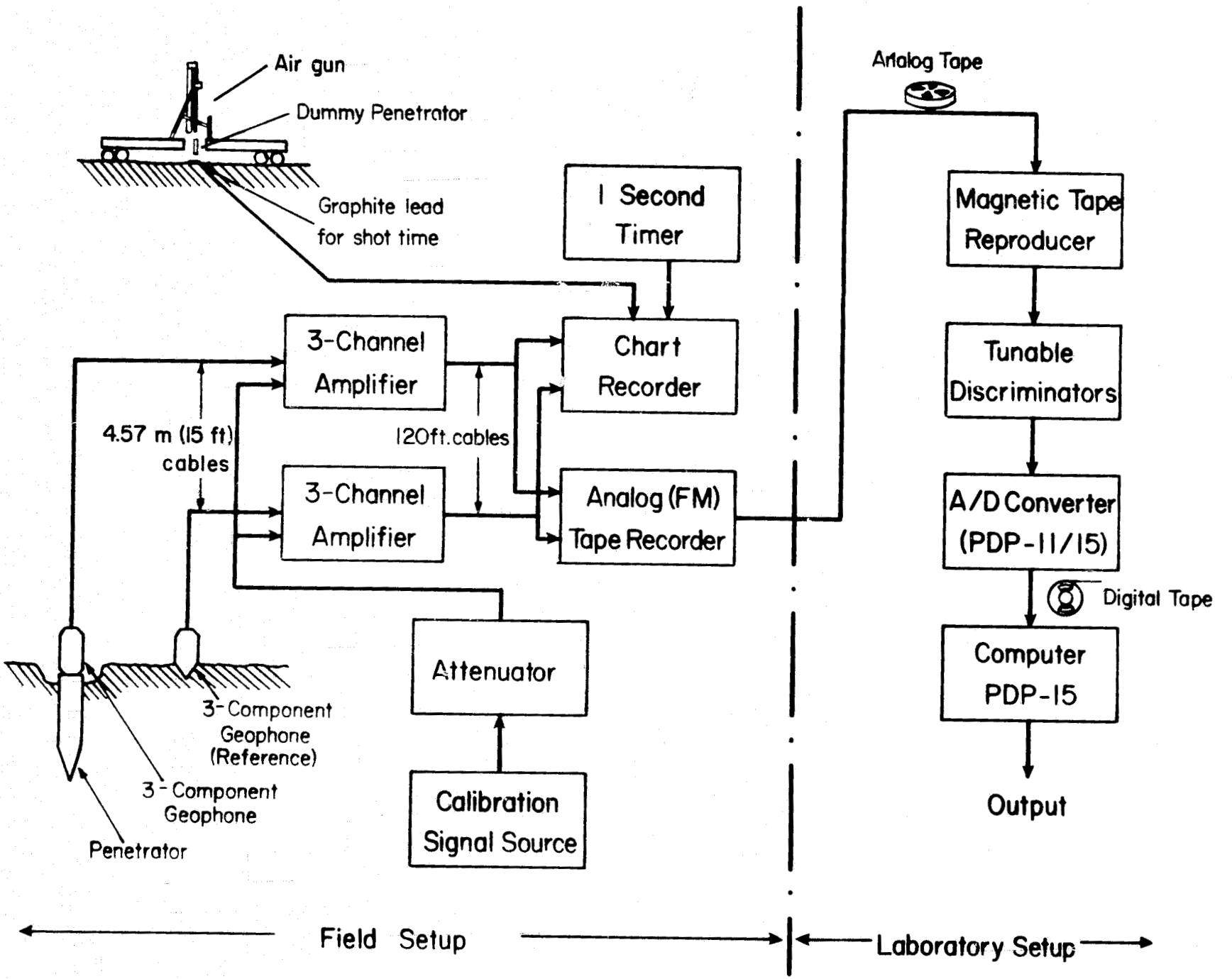

Figure 1.- Block diagram of experimental setup.

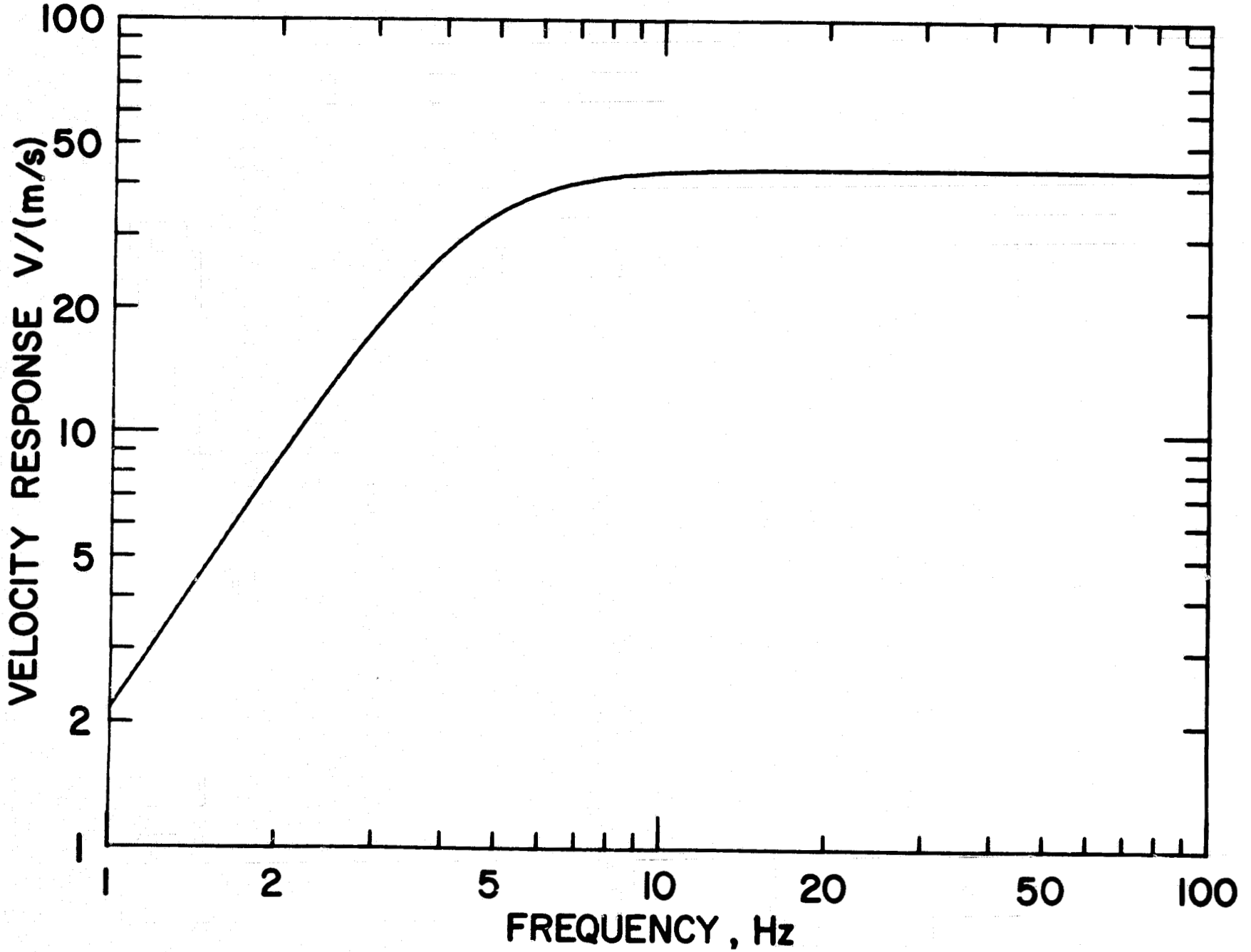

Figure 2.- Nominal response of Mark Products L-10, 4.5-Hz geophone.

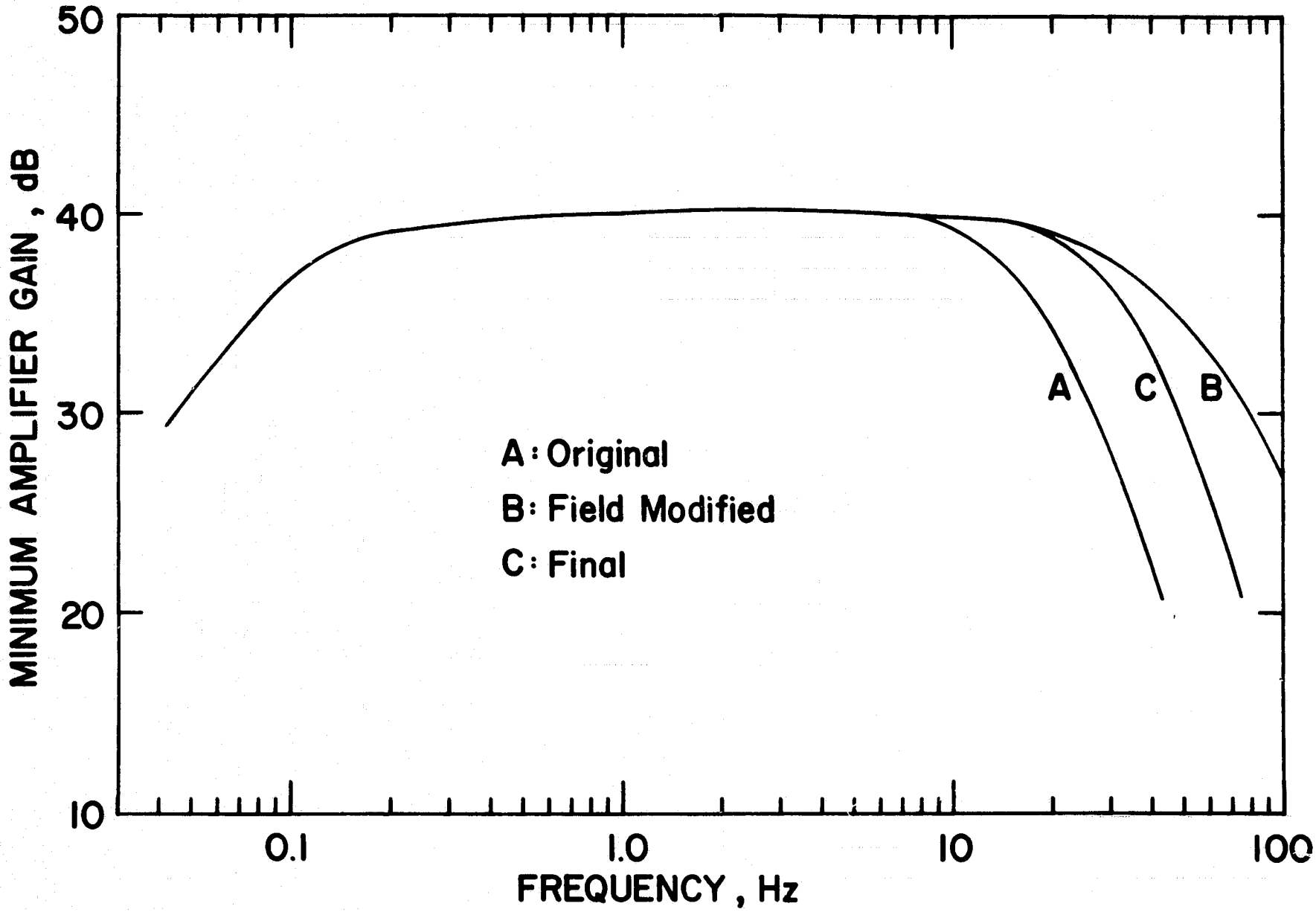

Figure 3.- Average measured response of amplifiers used in the experiment.

Dummy penetrators fired by an air gun served as sources to generate seismic waves. They were solid aluminum cylinders, 10.2 cm (4 in.) in diameter and 30.5 cm (12 in.) long. They were fired at a speed of 150 m/sec (±5%) vertically into the ground at distances ranging from 91 m (300 ft) to 274 m (900 ft) from the geophones. All the dummy firings were made along a line perpendicular to the line connecting the locations of the penetrator and the reference to maintain equal distances to both of the geophone assemblies for each shot. A thin graphite rod (a pencil lead) placed on the ground directly in the path of the penetrator and connected to an event marker was used to indicate on the chart recorder the time of impact of the penetrator.

Sine-wave and square-wave function generators combined with an attenuator provided calibration signals for the amplifier/recorder system. Ten-hertz sine waves of known amplitude were fed into the inputs of the amplifiers, and were recorded on magnetic tapes to obtain proper overall gain through the discriminator output. A 1-sec timer was added to the setup to place time marks on an event marker of the chart recorder for the White Sands test after it was learned during the Tonopah test that the fluctuation in the line frequency from a portable power generator caused large fluctuations in the chart speed.

The analog magnetic tapes were played back on a Bell and Howell VR-3700B magnetic tape recorder/reproducer using direct-reproduce amplifiers. The playback was normally done at twice the recording speed to reduce processing time. The reproduced signals were then demodulated through EMR-4142 tunable discriminators. The discriminator output was adjusted using the field-recorded 10-Hz calibration signals so that the overall system gain was precisely calibrated. The high-cut frequency of the discriminators was normally set to 100 Hz to reduce aliasing in digitized signals. This corresponded to 50 Hz in real time.

The demodulated signals were then fed into an Adac 12-bit analog-to-digital converter controlled by a combined PDP-11/PDP-15 computer, and were digitized at a rate of 400 samples/sec, corresponding to a real-time rate of 200 samples/sec. The digitized data were recorded on magnetic tapes. Finally, the digitized data were used to perform cross-spectral analysis using a PDP-15 computer.

III. FIELD MEASUREMENT

Tonopah Test

The first series of tests was conducted on a dry-lake bed located in a playa in the Sandia Laboratories Test Range about 50 km (31 miles) southeast of Tonopah, Nevada (approximate coordinates 37°51'N, 116°44'W), representing unconsolidated sediments. Figure 4 shows a section of the topographic map covering the area. The entire test setup, including the seismic signal sources, was located on the lake bed and was at least several hundred meters from the edges of the lake bed or any other irregularities. The test arrangement on the lake bed is shown schematically in figure 5. An analysis by Woodward-Clyde Consultants, of a soil core sample in the area (unpublished

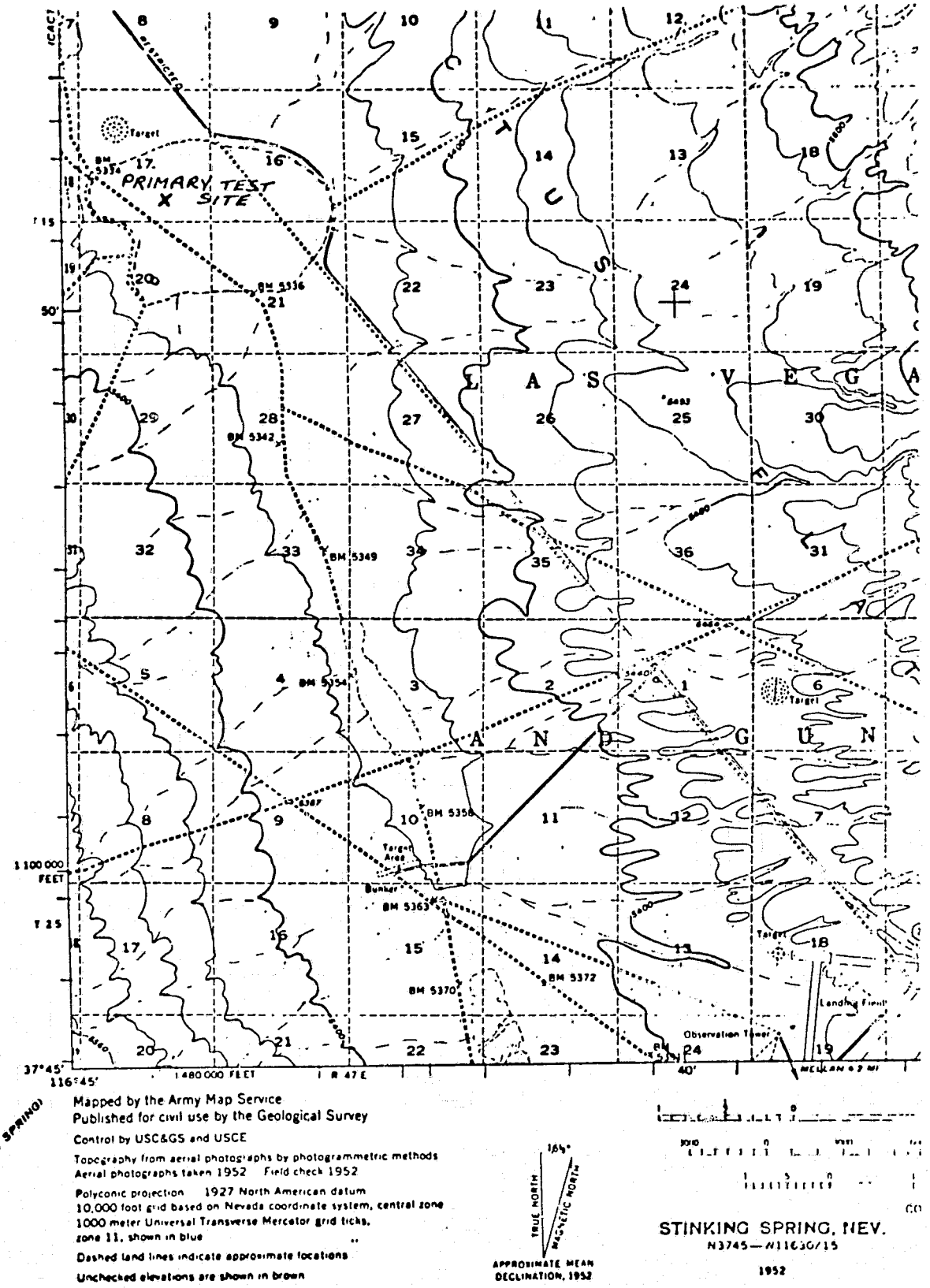

Figure 4.- A section of topographic map showing the location of the Tonopah test site on a dry-lake bed.

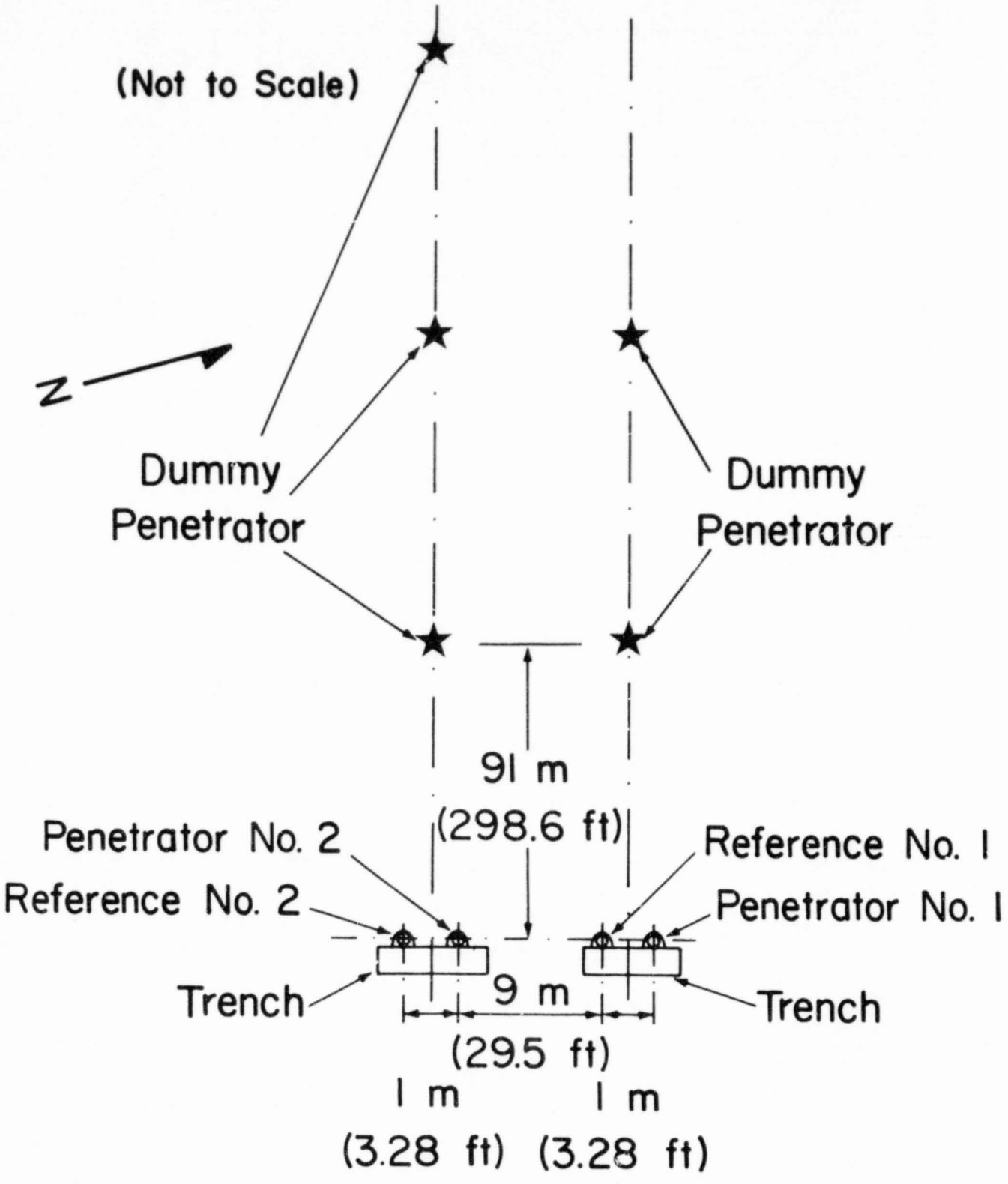

Figure 5.- Test arrangement on a dry-lake bed.

data) shows the following sequence of sediments: from the surface, 0.3 m (0.98 ft) of sand; 0.8 m (2.6 ft) of silty clay; 1.5 m (4.9 ft) of clayey sand; 0.3 m (0.98 ft) of sand; and at least 1 m (3.28 ft) of silty sand. The dry density of the sediments ranges from 1.47 to 1.76 g/cm^3.

The test was conducted as follows: A half-scale penetrator was fired into the ground at a speed of 150 m/sec (±5%) using a Sandia Laboratories air gun. The penetrator was a steel cylinder 6.35 cm (2.5 in.) in diameter and 61.0 cm (24 in.) long with a pointed nose cone; the penetrator did not contain geophones when it was fired. The firing embedded the penetrator to a depth of 250 cm (8.2 ft) at its aft end. The initial firing of the penetrator was monitored at three different distances by two triaxial heophone assemblies (only the vertical and the longitudinal horizontal axes were used) and an additional, vertical-component geophone without an amplifier. This was done to obtain estimates of the seismic signal strength to be expected from the later dummy firings, and also to obtain seismic travel-time information, from which to deduce the near-surface seismic velocity structure.

After the penetrator was embedded, a trench was dug on one side of the penetration hole using a backhoe down to the level of the aft end of the penetrator. The sediment surrounding the main body of the penetrator was not disturbed. The trench was 65 cm (2.1 ft) wide, 250 cm (8.2 ft) deep, 335 cm (11 ft) long at the surface, and 220 cm (7.2 ft) long at the bottom. The penetrator was found to be tilted by about 8°. A geophone assembly was mounted to the aft end of the penetrator using an adapter bracket with a 10° wedge to bring the geophone assembly within 2° of vertical alignment (see fig. 6(a)). Another geophone (reference geophone) assembly was installed inside a recessed hole on the same side of the trench as the penetrator and at about the same depth as the other geophone assembly on the penetrator. It was firmly coupled to the ground using plaster of paris. The horizontal separation between the geophones was 1 m (3.28 ft) which was more than 10 times the thickness of the zone of deformation caused by the impacting penetrator.

While the trench was still open, a dummy penetrator was fired into the ground at a distance of 91 m (300 ft), and the resulting seismic signals were recorded. This was done to test the mounting of the geophone assemblies while they were still accessible, and at the same time to observe the effect of the open trench on the observed seismic signals. The dummy penetrator penetrated to a depth of about 75 cm (2.5 ft) at its aft end.

A steel pipe with an outer diameter of 11.4 cm (4.5 in.) was then placed over the instrumented penetrator to protect the penetration hole, and the trench was back-filled and dry-compacted. The entire amount of soil originally taken out of the trench was used for the filling, and upon completion, the surface of the ground was level with the surrounding area. Thus, the dry compaction achieved the same average density for the filled soil as the surrounding, undisturbed sediments. The steel pipe was then removed, leaving an open penetration hole.

Two additional dummy penetrators were fired to this first instrumented penetrator at distances of 91 m (300 ft) and 183 m (600 ft), and the seismic

(a) Mounted on penetrator No. 1 with a 10°-wedge adapter.

(b) Tonopah test.

Figure 6.- Reference geophone assembly.

signals were recorded. It was found that the transverse-component reference geophone was not functioning properly, apparently because the reference geophone assembly had been tilted excessively during the dry compaction of the trench. Therefore, it was decided to repeat the test, paying more attention to keeping the reference geophone undisturbed during compaction.

A second penetrator was fired at a distance of 10 m (32.8 ft) from the first penetrator along the extension of the line from the first penetrator to the reference at the same speed as before. It penetrated to a depth of 260 cm (8.5 ft) at its aft end, and embedded at less than 1° tilt. As before, a trench was dug to expose the aft end of the penetrator and a geophone assembly was mounted to the aft end of the penetrator using an adapter bracket without a wedge.

The reference geophone assembly was installed with more care than previously. The geophone assembly was first mounted on a flat aluminum plate, 34 cm × 29 cm × 6.4 mm (13.4 × 11.4 × 0.025 in.). Four 19-mm diameter (0.75-in.) bolts were attached to the four corners of the plate to increase the surface area through which the assembly was to be coupled to the surrounding medium. A recessed hole, approximately 50 cm (19.7 in.) wide, 40 cm (15.7 in.) deep, and 50 cm (19.7 in.) high, was made on the trench wall as before at a distance of 1 m (3.28 ft) from the penetrator. The floor of the hole was carefully cleaned to remove loose soil. Three 19-mm (0.75-in.) diameter, 15-cm (6-in.)-long lag bolts were driven into the floor of the recessed hole and the top ends of the bolts were leveled. The plate assembly with the geophones was then placed on top of the bolts and was cemented to the floor using plaster of paris; the plaster of paris covered the edges of the plate, including the four attached bolts, and filled the entire space between the floor and the bottom of the plate (see fig. 6(b)).

As before, one dummy penetrator was fired with the trench still open at a distance of 91 m (300 ft). After the trench was carefully back-filled and compacted, three dummy penetrators were fired at distances of 91 m (300 ft), 183 m (600 ft), and 274 m (900 ft), and the seismic signals were recorded. Because there appeared to be very little high-frequency ground noise in the recorded data we decided to extend the high-frequency response of the filters built into the amplifiers. Therefore, we modified the amplifiers as described earlier (fig. 2), and fired two additional dummy penetrators at 183 m (600 ft) using two different gain settings.

While we were conducting this experiment, another unrelated series of tests was being performed nearby; it involved the firing of artillery guns. These guns, about 2.5 km (1.6 miles) east of our setup, generated seismic signals observable at our site. Air-coupled surface wave signals generated by two of these firings were recorded to provide supplementary data.

White Sands Test

The second series of tests was conducted in a lava field located at the southwest end of the Malpais lava flow about 40 km (25 miles) northwest of

Tularosa, New Mexico, just inside the eastern boundary of the White Sands Missile Range (approximate coordinates 33°19'N, 106°19'W), representing volcanic rocks. Figure 7 shows a section of the topographic map covering the area. At this location, volcanic rocks of basaltic composition are exposed, forming rock "fingers" extending out of the main body of the lava bed. The rocks have an approximate porosity of 30%. The lava beds are at least several meters thick, and consist of a large number of individual flows, each with a thickness of 10 to 20 cm (3.9 to 7.9 in.) and often separated from one another by large cavities.

Since the main body of the lava bed was inaccessible to the vehicle carrying the air-gun equipment, the one-half-scale penetrators were fired into the exposed rock "fingers." Dummy penetrators, used to generate seismic waves, were fired into the desert alluvium lying adjacent to the lava bed. Figure 8 is a schematic map of the area showing the test setup.

The test was conducted as follows: prior to the firing of the first penetrator into the lava bed, the two geophone assemblies were installed with a 64-cm (2-ft) separation between them at the places where the penetrator and the reference geophones were to be placed. Then, the first dummy penetrator was fired into the desert alluvium at a distance of 91 m (300 ft), and the seismic signals were recorded. This was done to determine how the signals from two similarly installed reference geophones compare with each other in view of the apparent nonuniformity of the lava bed in the area.

The first penetrator was fired into the lava bed at a speed of 150 m/sec (±5%). It was embedded with a tilt of 21° from vertical, exposing a few centimeters of its aft end above the surface of the rock. The firing was again monitored at three different distances to obtain travel-time data.

After the penetrator was embedded, a geophone assembly was mounted to its aft end using an adapter bracket (see fig. 9(a)). This adapter bracket was different from those used for the Tonopah test, as it allowed a variable adjustment of the mounting angle by use of a ball-and-plates mechanism; thus the geophone assembly could be mounted vertically regardless of the angle of tilt of the penetrator. The reference geophone assembly was firmly installed on the surface of the lava bed using plaster of paris at a distance of 56 cm (1.8 ft) from the penetrator (see Fig. 9(a)).

Three dummy penetrators were fired — at distances of 91 m (300 ft), 183 m (600 ft), and 274 m (900 ft) — and the seismic signals recorded. For the last shot, however, the tape recording was missed because of a failure in radio communications between the firing crew and the recording crew.

The test was repeated using another penetrator, which was fired into another outcrop at a distance of 5.2 m (17 ft) from the first one. It completely penetrated the first layer of the lava sequence, and embedded in the second layer with its aft end exposed inside a cavity which existed about 10 cm (3.9 in.) below the surface. It was tilted by 10° from the vertical. A geophone assembly was mounted to the aft end of the penetrator using the same 10°-wedge adapter bracket that had been used in the Tonopah test (see

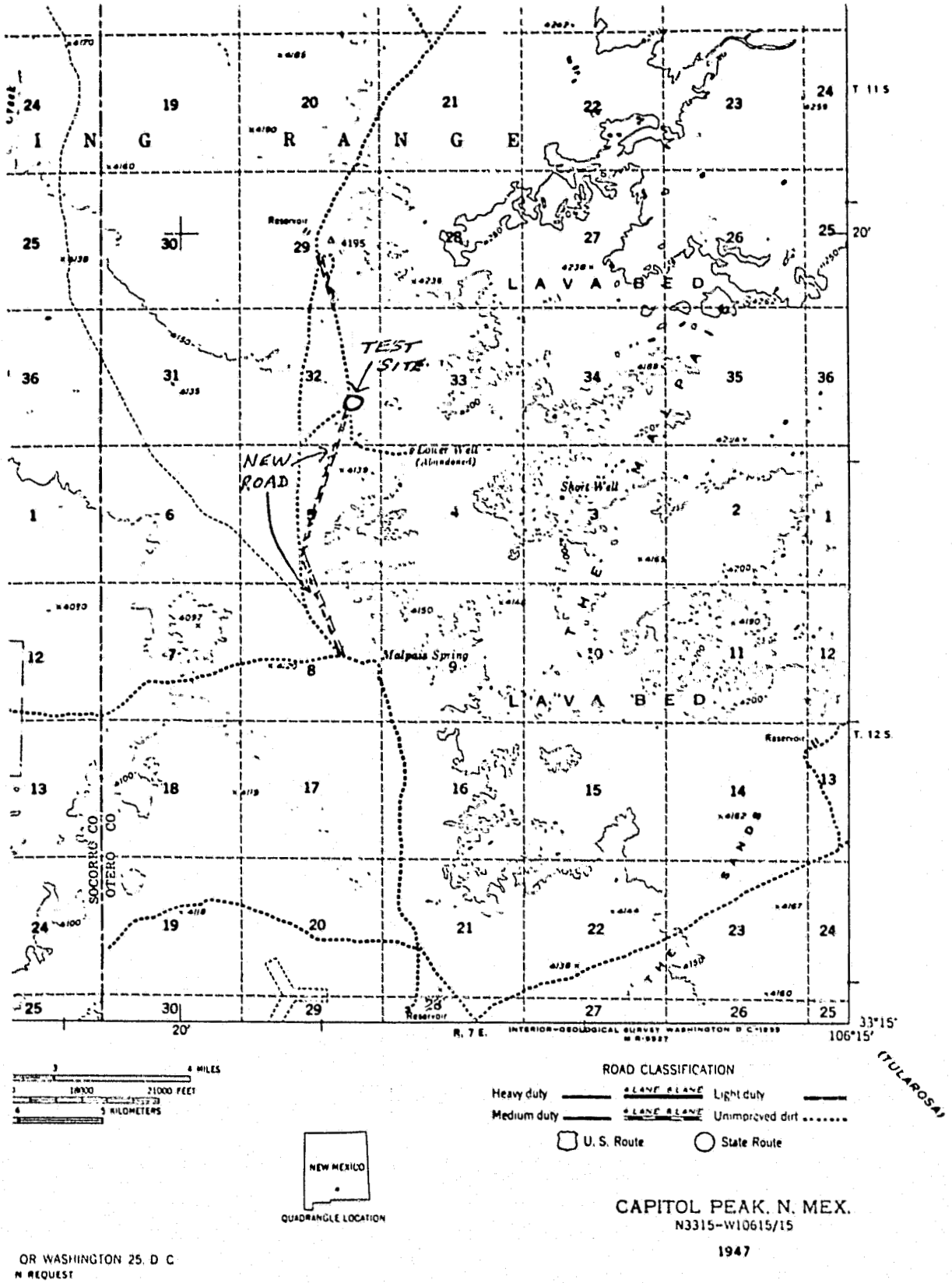

Figure 7.- A section of topographic map showing the location of the White Sands test site in a lava field.

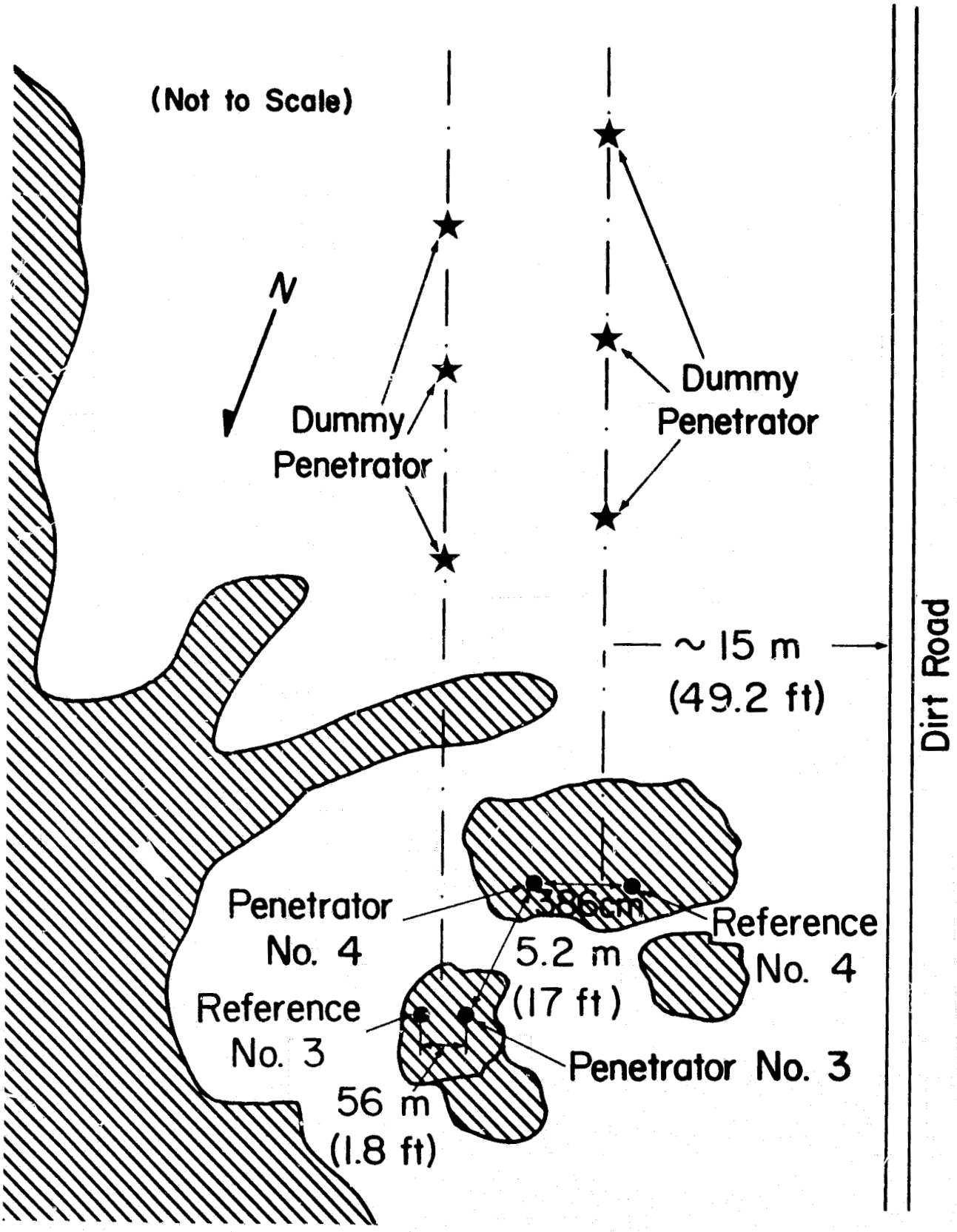

Figure 8.- Test arrangement in the Malpais lava field, White Sands; shaded areas represent exposed lava beds.

fig. 9(b)). The ball-type adapter, which had been used with the preceding penetrator, was not used this time because it appeared that the ball-adapter/geophone system had a mechanical resonance at a frequency of about 90 Hz; the resonance was clearly visible on the seismic records. The reference geophone assembly was installed 386 cm (12.7 ft) away on another outcrop that looked more stable than the one on which the penetrator rested.

Four dummy penetrators were fired into the desert alluvium with this setup at distances of 91 m (300 ft), 91 m (300 ft), 183 m (600 ft), and 274 m (900 ft). The first dummy firing was not recorded on a magnetic tape because of a tape recorder malfunction. Finally, to confirm our suspicion that the ball-type adapter allowed a high-frequency resonance to occur, the adapter was replaced by the ball-type adapter, and the signals from the final dummy penetrator firing at a distance of 183 m (600 ft) were recorded.

Data Obtained

Table 1 lists the data obtained during the field experiment. Copies of the chart recordings are provided in the appendix.

IV. DATA ANALYSIS AND RESULTS

Travel Times and Near-Surface Structures

Copies of selected chart recordings, arranged according to distance, are shown in figures 10 and 11 for the Tonopah test and the White Sands test, respectively. In both tests, initial body-wave arrivals are followed by a large-amplitude surface wave train. The surface-wave train is simpler and shorter for the White Sands site than for the Tonopah site, possibly indicating that no low-velocity, near-surface channel exists at the White Sands site. A low-velocity, near-surface channel probably is responsible for the prolonged surface-wave train with low group velocity that is observed at the Tonopah site. The air-coupled surface wave, which travels at the speed of sound in the air, is also visible as a high-frequency arrival on recordings from both sites.

The travel times of the initial arrivals were read from the chart records and, after being corrected for chart speed variations, plotted in figures 12 and 13. The travel-time curve for the Tonopah site consists of two distinct straight-line segments, representing two velocities: 0.6 km/sec and 2.0 km/sec. The 13-msec offset of the first segment from the origin is probably caused by the delay between the instant when the penetrator hit the ground surface (thus breaking the graphite rod) and the time when the penetrator began to impart a significant amount of energy into the ground at some depth below the surface. Assuming, as a first approximation, a constant deceleration of the penetrator during its 3-m (9.8 ft) path through the ground before stopping, a penetrator with an initial speed of 150 m/sec penetrates 1.3 m (4.3 ft) in the first 13 msec of penetration, and takes 40 msec to stop.

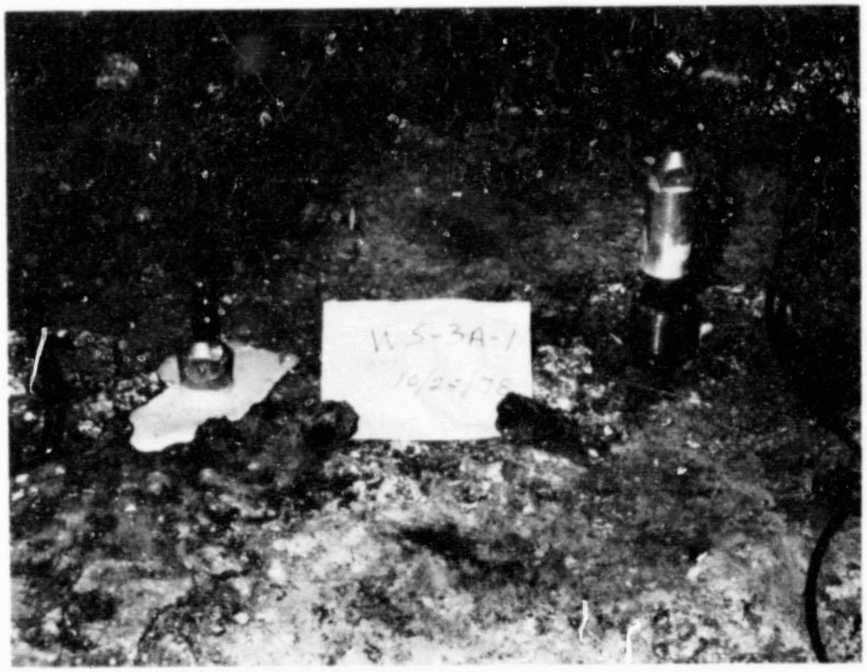

(a) Assembly mounted on penetrator No. 3 with a ball-type adapter bracket (right), and the reference geophone assembly installed on the ground (left); White Sands test.

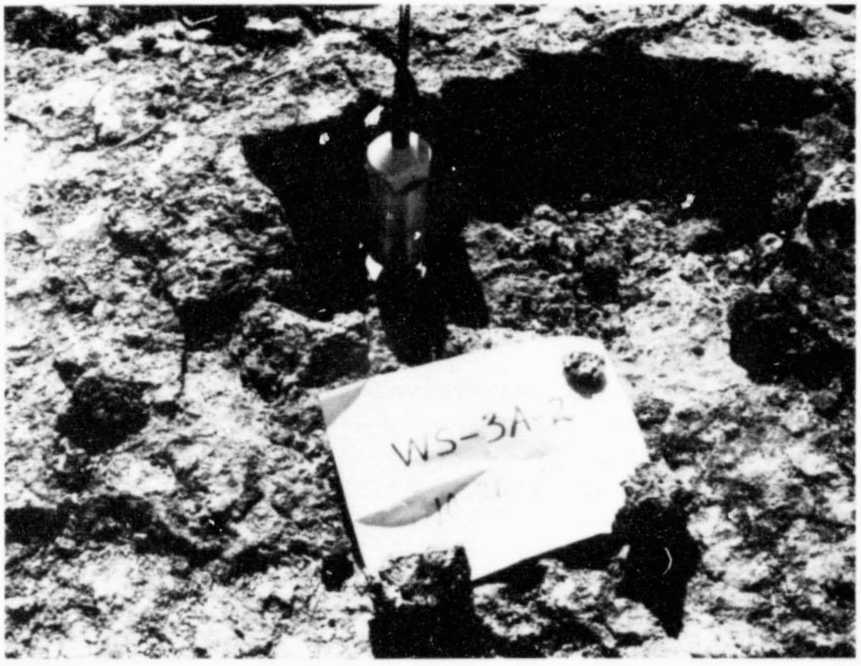

(b) Assembly mounted on penetrator No. 4 with a 10°-wedge adapter bracket.

Figure 9.- Mounting of geophone assembly on penetrators Nos. 3 and 4.

TABLE 1.- RECORDED SEISMIC DATA.*

Date	Time (hr:min)	Source[b]	Distance (m)	Remarks
Tonopah Test				
Oct. 9	12:20	P-1	30,46,61	
Oct. 10	13:45	D-1	91	open trench
	15:45	D-2	91	
	17:04	D-3	183	
Oct. 11	14:00	P-2	122,152,183	
Oct. 12	09:33	G-1	~2500	
	09:36	D-4	91	open trench
	11:56	D-5	91	
	12:30	D-6	183	
	13:27	G-2	~2500	
	13:29	D-7	274	
	14:45	D-8	183	modified filter, low gain
	15:04	D-9	183	modified filter
White Sands Test				
Oct. 25	13:40	D-10	91	two references
	15:28	P-3	15,30,61	
	16:49	D-11	91	
	17:19	D-12	183	
Oct. 26	10:07	P-4	23,46,46	one geophone off shooting line
	14:57	D-15	91	
	15:16	D-16	183	
	15:44	D-17	274	
	16:21	D-18	183	with ball-type adapter

*Penetrator firing signals were recorded on chart recorder only.
[b]P=penetrator; D=dummy penetrator; G=gun firing.

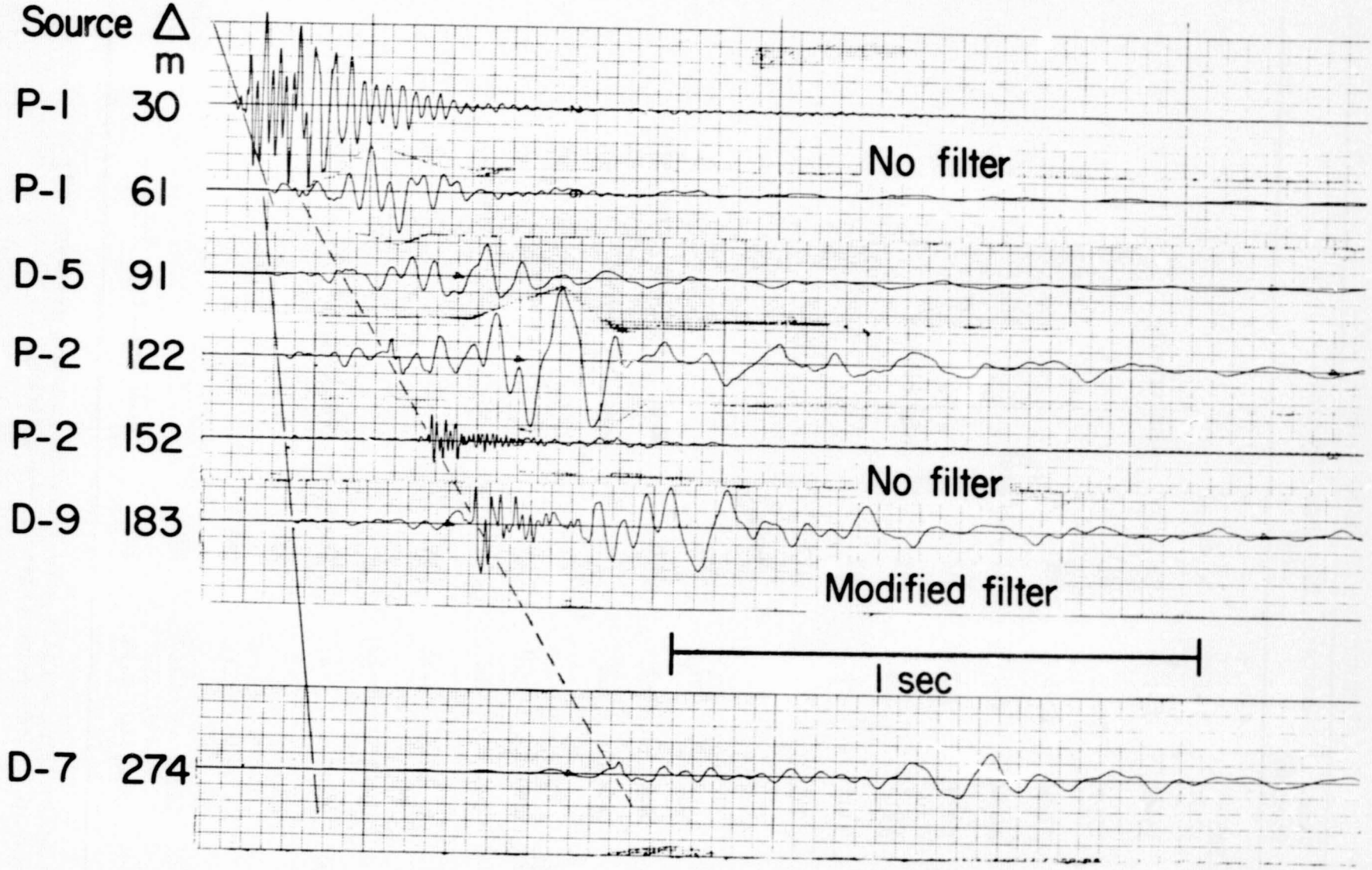

Figure 10.- Selected seismic record sections for the Tonopah site. The seismograms shown are of vertical component only. The solid line indicates the beginning of the initial P-wave arrivals, and the broken line indicates the beginning of high-frequency, air-coupled surface waves. Identification of signal sources and distances are given in the left margin.

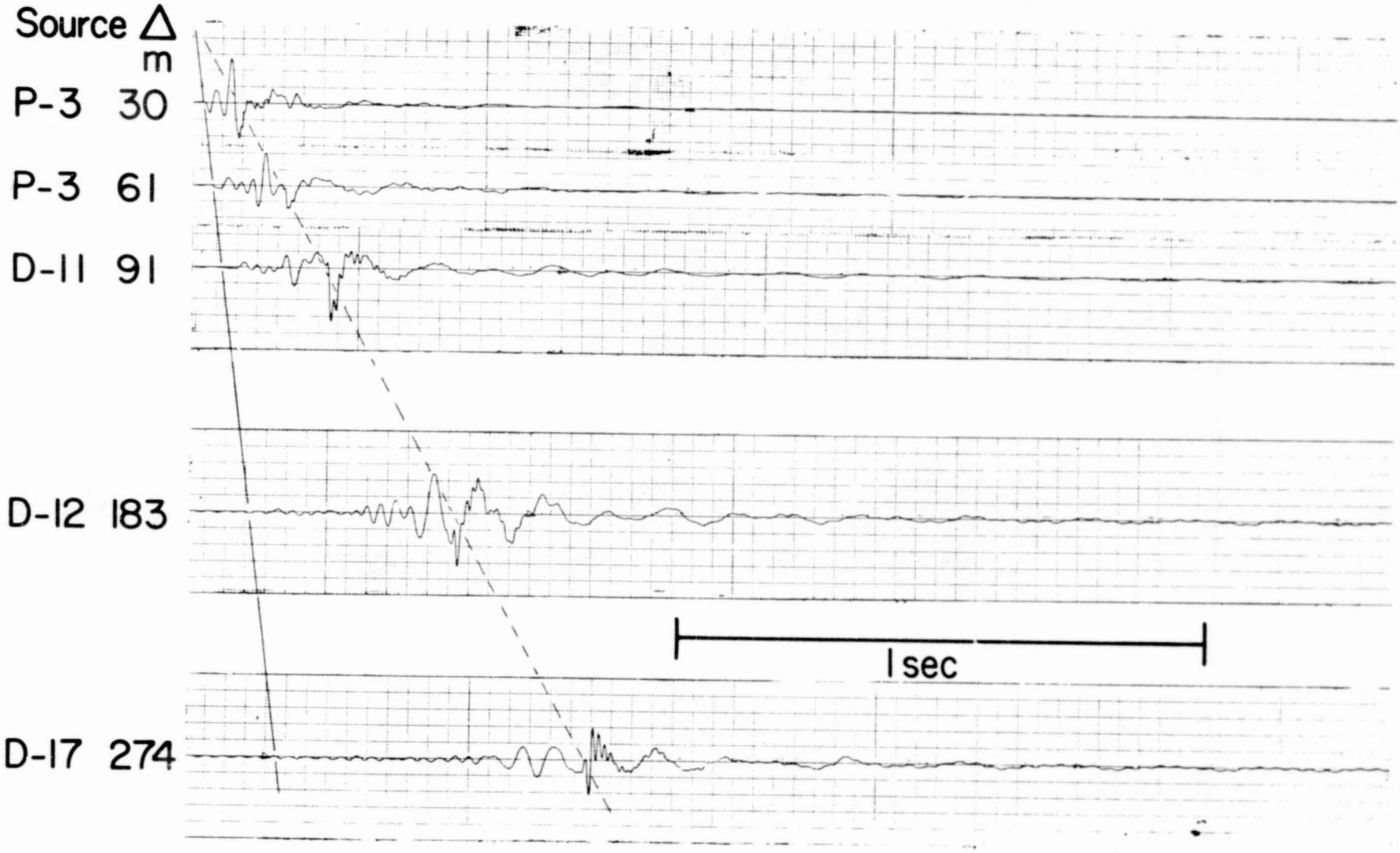

Figure 11.- Selected seismic record sections for the White Sands test. The seismograms shown are of vertical component only. (See fig. 10 caption for other explanations.)

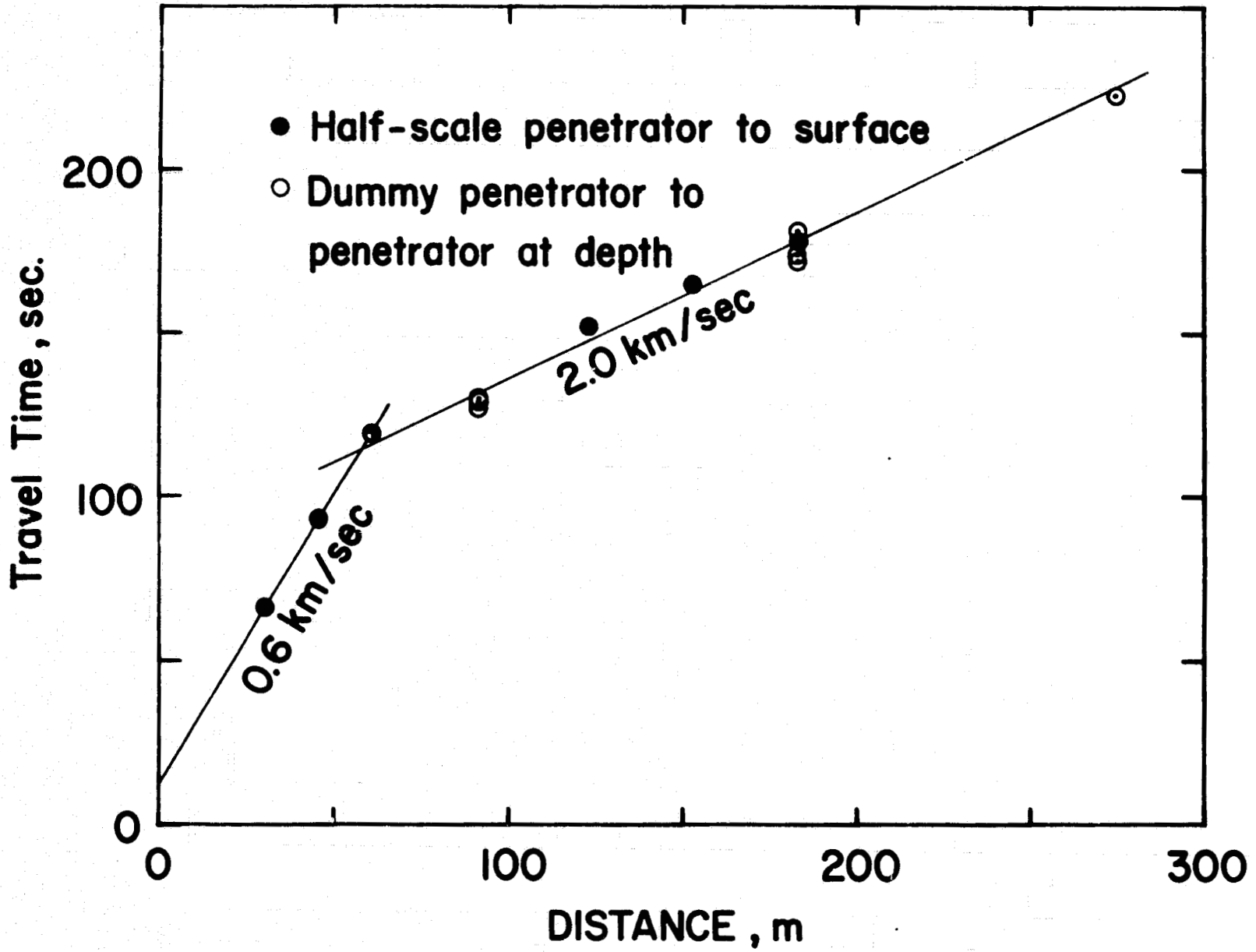

Figure 12.- Travel time-distance diagram for the Tonopah site. The dummy-penetrator signals tend to arrive earlier because the initial time delay is less than those for the penetrator shots, and the geophone is at depth for these shots.

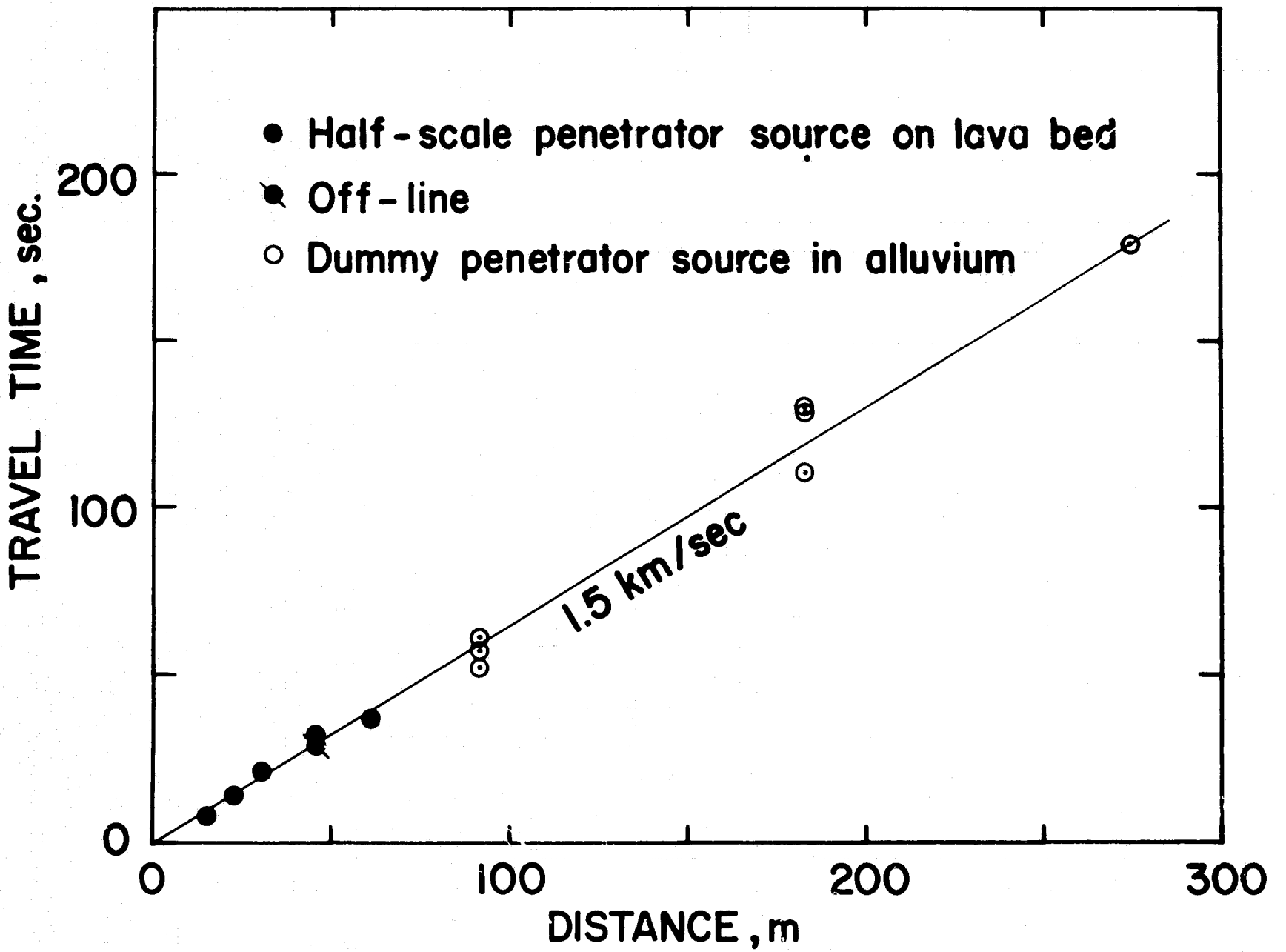

Figure 13.- Travel time-distance diagram for the White Sands site. The off-line data represent a transmission mostly through the lava bed. Others are from lava bed to alluvium.

For the dummy penetrators, the deceleration was more rapid because of their flat front faces. Again assuming a constant deceleration during its 1-m (3.28-ft) path through the ground before stopping, a dummy penetrator with an initial speed of 150 m/sec stops in about 13 msec. In calculating the thickness of the top layer, therefore, the following assumptions are made: for the penetrator shots, the source is assumed to be at a depth of 1.3 m (4.3 ft) with an initial delay of 13 msec; for the dummy shots, the source is assumed to be at a depth of 0.4 m (1.3 ft) with an initial delay of 4 msec. Also taken into account are the depths of the detectors: zero for the penetrator shots, and 2.5 m (8.2 ft) for the dummy shots. Assuming flat-lying layers, the calculations suggest that the near-surface structure at the Tonopah site consists of a 26-m (85-ft)-thick surface layer with a P-wave velocity of 0.6 km/sec overlying a layer of undetermined thickness with a P-wave velocity of 2.0 km/sec. What this 2.0 km/sec layer at a depth of 26 m (85 ft) represents cannot be determined from the seismic data alone.

The travel-time curve for the White Sands site can best be represented by a single straight line through the origin. From the slope of the line, we obtain 1.5 km/sec for the P-wave velocity of the surface layer. The thickness of this layer is at least 100 m (328 ft) if the P-wave velocity in the underlying layer is 2 km/sec or greater. There is little difference between the measured velocities along the paths that lie mostly in the lava bed and those along the paths through the desert alluvium. It is possible that the alluvium deposit is a thin layer covering an extension of the lava bed which lies underneath. We occupied this site immediately following a heavy rain that lasted several days. Therefore, an alternative explanation may be that the 1.5-km/sec velocity represents water-saturated desert alluvium deposit that lies over a dry alluvium deposit of lower seismic velocity. If so, its thickness may be much less. However, the simple surface-wave train of high group velocity described above does not favor this latter interpretation.

Comparison of Signal Characteristics

A visual comparison of seismic signals from the penetrator and the reference reveals very little difference in most respects at both sites (see seismograms in appendix). The signal waveforms are nearly identical throughout the wave train, including both body-wave and surface-wave arrivals. There are no visible signs of phase distortion for the geophones on the penetrator compared with the reference. The amplitudes of the signals are also nearly identical for the most part.

A closer observation, however, reveals a few minor differences. For the Tonopah test, the longitudinal horizontal component geophone on the penetrator tends to show slightly reduced amplitude relative to the reference for waves of frequencies higher than about 10 Hz. However, the difference is very slight, amounting to only a few decibels in the 20 to 30 Hz range. On the other hand, for the White Sands test, the longitudinal horizontal component geophone on the penetrator tends to show a slightly larger amplitude for waves of frequencies higher than about 20 Hz. For the most part, however, the observed differences in amplitudes are within the uncertainty of the

instrument response, which is estimated to be about ±1 dB. (The vertical component signals from gun firing No. 1 and the dummy penetrator shots Nos. 4 and 5, all of which were recorded in the morning of October 12, seem to be exceptional, showing smaller signals for the penetrator-mounted geophone. Circumstances indicate that the amplifier gain may have been erroneous.)

Things are clearly different for waves of very high frequencies. When operated with the filters open for high frequencies, a large difference in signals of frequencies higher than about 50 Hz was observed. The difference, however, does not seem to represent the intrinsic difference in ground coupling between the penetrator and the reference. This was particularly evident when we compared the signals from two similarly installed reference geophones in the White Sands tests. Clearly different high-frequency signals were observed when we moved geophones from one flow unit to another, even when the distance moved was only a few centimeters. It appears that the location of the geophone on a particular flow unit or a section of a flow unit actually makes a significant difference in the signals at these very high frequencies.

Cross-Spectral Analysis

We have performed cross-spectral analysis on the digitized signals in order to obtain more quantitative comparison between signals recorded on the penetrator and on the reference. Specifically, we have computed (1) the power-spectral density (PSD) ratios, (2) the coherence spectra and (3) the cross-phase spectra for all respective pairs of recorded signals. The coherence and phase spectra of signals A and B are defined by Kanasewich (ref. 7, pp. 115-116):

$$\text{Coherence } (\omega) = \frac{(\text{cospectrum of A and B})^2 + (\text{quadrature spectrum of A and B})^2}{(\text{power spectrum of A}) \times (\text{power spectrum of B})}$$

$$\text{Phase } (\omega) = \tan^{-1} \frac{\text{quadrature spectrum of A and B}}{\text{cospectrum of A and B}}$$

The spectra were computed for the entire length of the signals (generally 7.5 sec) using a Parzen window with a maximum width of ±128 sampling points. With the digitization sampling rate of 200 samples/sec, this gives a frequency resolution of 0.78 Hz and a one-half power band width of ±1.00 Hz. Tables 2-4 list the ranges of computed PSD ratio, coherence, and phase difference, respectively, within three frequency bands of 3 to 10, 10 to 20, and 20 to 30 Hz. We limit the analysis in this range because the signal power is generally very small outside the range, thus increasing the uncertainty of cross-spectral estimates. Some representative computed spectra are shown in figures 14-17.

The coherence between the penetrator and the reference signals, table 3, is extremely high. For frequencies below 10 Hz, it is generally greater than 99%. The apparently low lower-limit values for the White Sands data for this frequency range occur only at the low-frequency end of the spectrum, where the spectral power is very small. Excluding this value, the remaining values of coherence for the White Sands data are as high as those for the Tonopah data. Somewhat lower values of coherence are observed at frequencies above 10 Hz.

TABLE 2.- RANGES OF OBSERVED POWER SPECTRAL RATIOS.

Geophones	Source	Vertical 3-10 Hz	Vertical 10-20 Hz	Vertical 20-30 Hz	Longitudinal Horizontal 3-10 Hz	Longitudinal Horizontal 10-20 Hz	Longitudinal Horizontal 20-30 Hz
P-1/Ref	**D-1**	0.0~+0.3	-0.4~+0.7	-1.3~-0.3	-0.1~+0.4	-1.1~+0.4	-4.9~-0.6
	D-2	-0.1~+0.3	-0.5~+0.7	-0.9~+0.2	0.0~+0.3	+0.1~+0.8	-2.4~+2.0
	D-3	-0.1~+0.4	-0.2~+0.4	-2.6~-0.2	-0.5~+0.3	-1.1~+0.4	-2.7~+0.6
P-2/Ref	**D-4**	-3.8~-3.2	-5.7~-3.7	-6.2~-3.6	-0.4~+0.4	-0.9~+0.8	-4.0~-0.7
	D-5	-3.9~-3.4	-6.8~-3.7	-6.1~-3.4	-0.6~+0.2	-2.4~-0.4	-7.1~-0.8
	D-6	-0.6~+0.1	-1.0~+0.3	-2.4~+0.1	-0.8~+0.3	-6.0~-1.1	-6.9~-2.1
	D-7	-0.3~-0.1	-2.1~-0.2	-3.2~ 0.0	-0.5~+0.8	-7.4~ 0.0	-9.9~-0.9
	D-8	-0.3~+0.4	-0.8~+0.7	-1.4~+0.8	-0.9~+0.3	-6.4~-1.0	-6.4~-2.3
	D-9	-0.7~ 0.0	-1.2~+0.2	-1.8~+0.1	-1.0~+0.3	-6.2~-1.0	-6.4~-2.8
Tonopah Ave.*		-0.3~+0.2	-0.9~+0.4	-1.9~+0.1	-0.5~+0.4	-3.5~-0.1	-5.6~-0.8
P-3/Ref	**D-11**	-0.3~+0.4	-0.2~+0.3	-1.5~-0.7	+0.4~+2.3	+0.9~+3.6	+1.6~+6.4
	D-12	-0.6~+0.1	0.0~+1.4	-0.4~+1.5	-0.1~+2.3	+1.3~+4.3	+3.0~+9.0
P-4/Ref	**D-15**	-0.7~+0.9	-2.4~+0.2	-7.8~+5.7	-2.5~+1.6	+0.4~+2.6	-0.5~+5.8
	D-16	-0.1~+0.2	-1.5~ 0.0	-2.7~+1.6	-1.9~+0.9	+0.4~+1.2	-1.2~+2.8
	D-17	-0.3~+0.2	-4.5~-0.6	-5.9~+0.6	-0.5~+0.6	-3.2~+0.5	-4.9~+3.9
	D-18	-0.1~+0.4	-1.0~+0.4	-2.5~+1.2	-0.2~+1.0	+1.0~+2.8	+0.2~+5.5
W. S. Ave.		-0.4~+0.4	-1.6~+0.3	-3.5~+1.7	-0.8~+1.5	+0.1~+1.8	-0.3~+5.6
Ref/Ref	D-10	-0.5~+0.4	-3.3~-0.3	-3.4~-1.2	-0.2~+0.8	0.0~+0.9	0.0~+0.7
P-2/Ref	**G-1**	-3.6~-3.5	-5.2~-3.4	-5.0~+7.1			
	G-2	-0.5~-0.2	-1.2~ 0.0	-2.4~-0.8			

*excluding D-4 and D-5 results

TABLE 3.- RANGES OF OBSERVED COHERENCE.

Geophones	Source	Vertical 3-10 Hz	Vertical 10-20 Hz	Vertical 20-30 Hz	Longitudinal horizontal 3-10 Hz	Longitudinal horizontal 10-20 Hz	Longitudinal horizontal 20-30 Hz
P-1/Ref	D-1	99-100	99-100	95-100	99-100	98-100	54-98
	D-2	99-100	100-100	94 100	100-100	98-100	81-99
	D-3	100-100	98-100	89-100	99-100	97-100	31-94
P-2/Ref	D-4	99-100	94-100	96-100	99-100	86-100	81-97
	D-5	99-100	96-100	97-100	99-100	37-100	11-85
	D-6	100-100	93-100	84-100	100-100	50-100	12-88
	D-7	100-100	91-100	86-98	98-100	60-98	25-75
	D-8	98-100	94-99	84-99	97-100	52-100	26-84
	D-9	99-100	95-99	90-100	100-100	59-100	40-92
Tonopah Ave.		99-100	96-100	91-100	99-100	71-100	40-90
P-3/Ref	D-11	92-100	99-100	97-100	80-100	96-100	72-98
	D-12	94-100	96-100	96-100	84-100	97-100	10-98
P-4/Ref	D-15	85-100	97-100	32-96	43-99	97-100	47-94
	D-16	91-100	97-100	76-99	94-100	98-100	91-99
	D-17	97-100	98-100	66-9[illegible]	77-100	95-100	35-96
	D-18	94-100	97-100	75-100	99-100	98-100	91-98
W. S. Ave.		92-100	97-100	74-100	80-100	97-100	58-97
Ref/Ref	D-10	90-100	95-100	98-100	96-100	94-100	91-99
P-2/Ref	G-1	97-100	88-98	48-100			
	G-2	96-100	92-100	96-100			

TABLE 4.- RANGES OF OBSERVED PHASE DIFFERENCES.

		Vertical			Longitudinal horizontal		
Geophones	Source	3-10 Hz	10-20 Hz	20-30 Hz	3-10 Hz	10-20 Hz	20-30 Hz
P-1/Ref	D-1	+5~+6	0~+6	+1~+5	-4~+1	-5~ 0	-28~-3
	D-2	+4~+5	+3~+6	-6~+4	-5~+1	-13~-3	-27~+1
	D-3	+3~+6	-2~+5	-5~+4	-3~+1	-15~-3	-17~-1
P-2/Ref	D-4	+3~+5	+1~+9	-4~+3	-13~-9	-23~-5	-29~-3
	D-5	+4~+6	-2~+8	-13~-3	-12~-6	-93~ 0	-83~+34
	D-6	+5~+7	-4~+8	-17~+2	-12~-8	-18~+10	-47~-8
	D-7	+4~+6	-13~+5	-16~+12	-11~-9	-28~-10	-94~+8
	D-8	+4~+5	-3~+6	-26~-1	-13~-7	-17~+26	-94~-12
	D-9	+3~+5	-3~+6	-18~-2	-12~-8	-16~+13	-94~-7
Tonopah Ave.		+4~+6	-3~+7	-12~+3	-9~-5	-25~+3	-57~+1
P-3/Ref	D-11	-1~+4	+1~+4	+2~+7	-14~+17	+20~+36	-8~+86
	D-12	0~+6	-2~+2	+3~+14	-11~+15	+20~+29	+21~+86
P-4/Ref	D-15	-5~+3	-6~+1	-30~+86	-18~+12	-12~-1	-44~+27
	D-16	-1~+3	-4~+7	-9~+19	-13~-9	-8~+13	-11~+11
	D-17	-3~+2	-10~ 0	-26~+4	-16~-7	-6~+4	-15~+35
	D-18	0~+2	-4~+6	-12~+14	-10~-2	0~+15	-6~+22
W. S. Ave.		-2~+3	-4~+3	-12~+24	-14~+4	+2~+16	-11~+45
Ref/Ref	D-10	-1~+4	+1~+8	+1~+13	-17~-6	-5~+2	-2~+6
P-2/Ref	G-1	-5~-2	-11~-2	-94~-10			
	G-2	-6~-1	-7~+2	-26~-6			

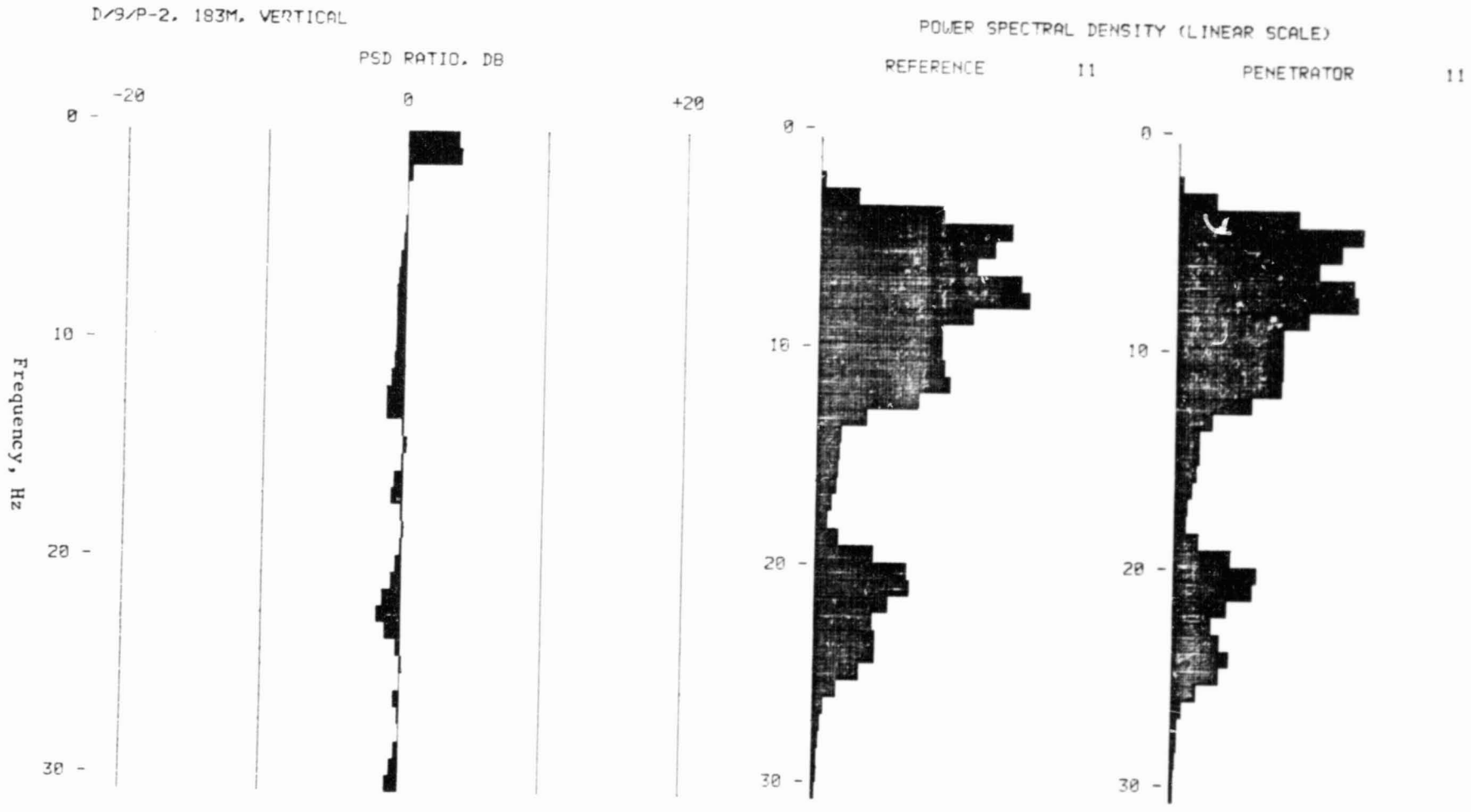

(a) Power spectral densities.

Figure 14.- Vertical power spectral densities, coherence, and cross-phase spectra of seismic signals from a dummy penetrator firing at a distance of 183 m (600 ft), observed by vertical-component geophone at the Tonopah test site, and the penetrator/reference PSD ratio.

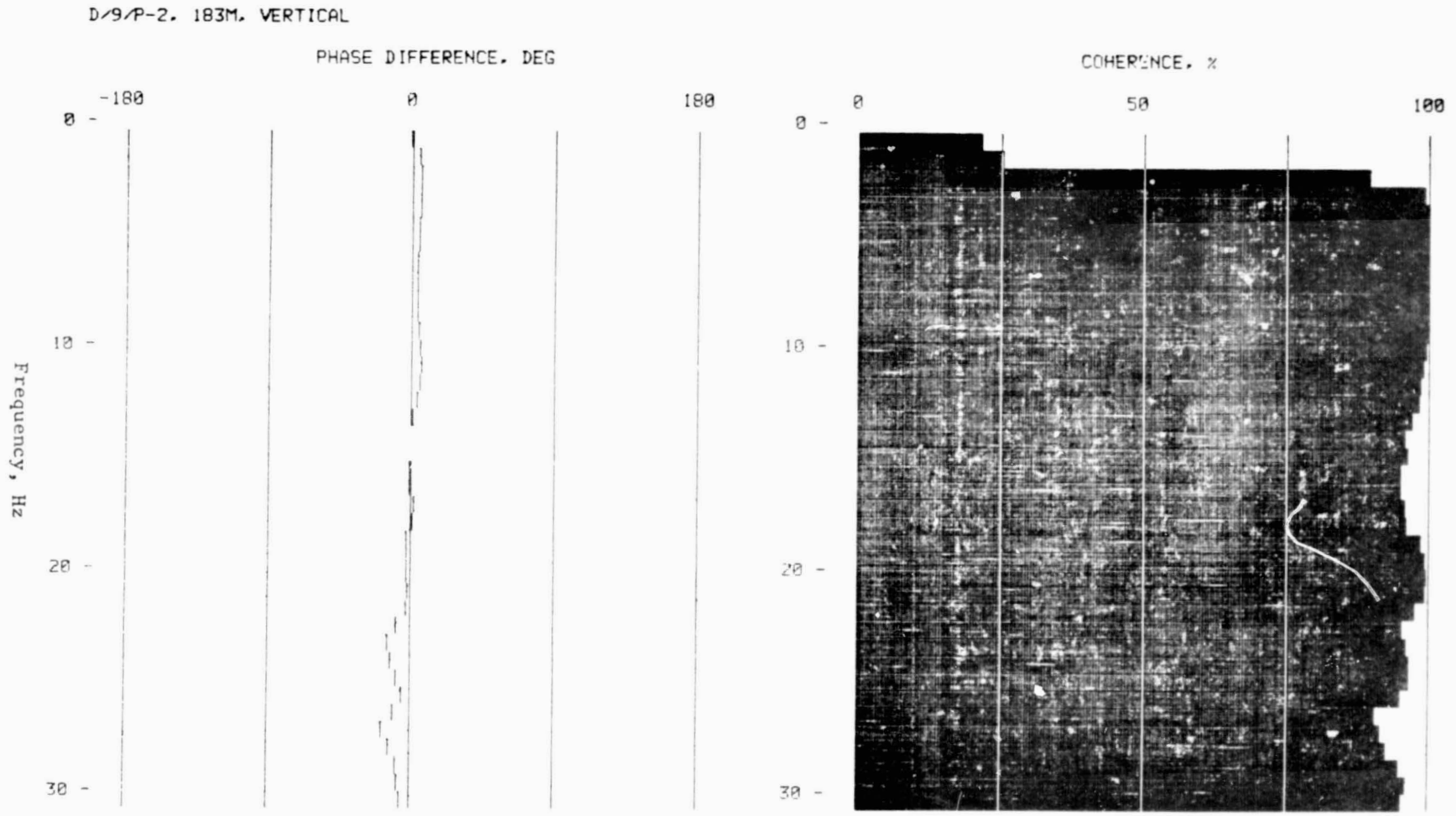

(b) Coherence and cross-phase spectra of the same pair of signals as figure 14(a).

Figure 14.- Concluded.

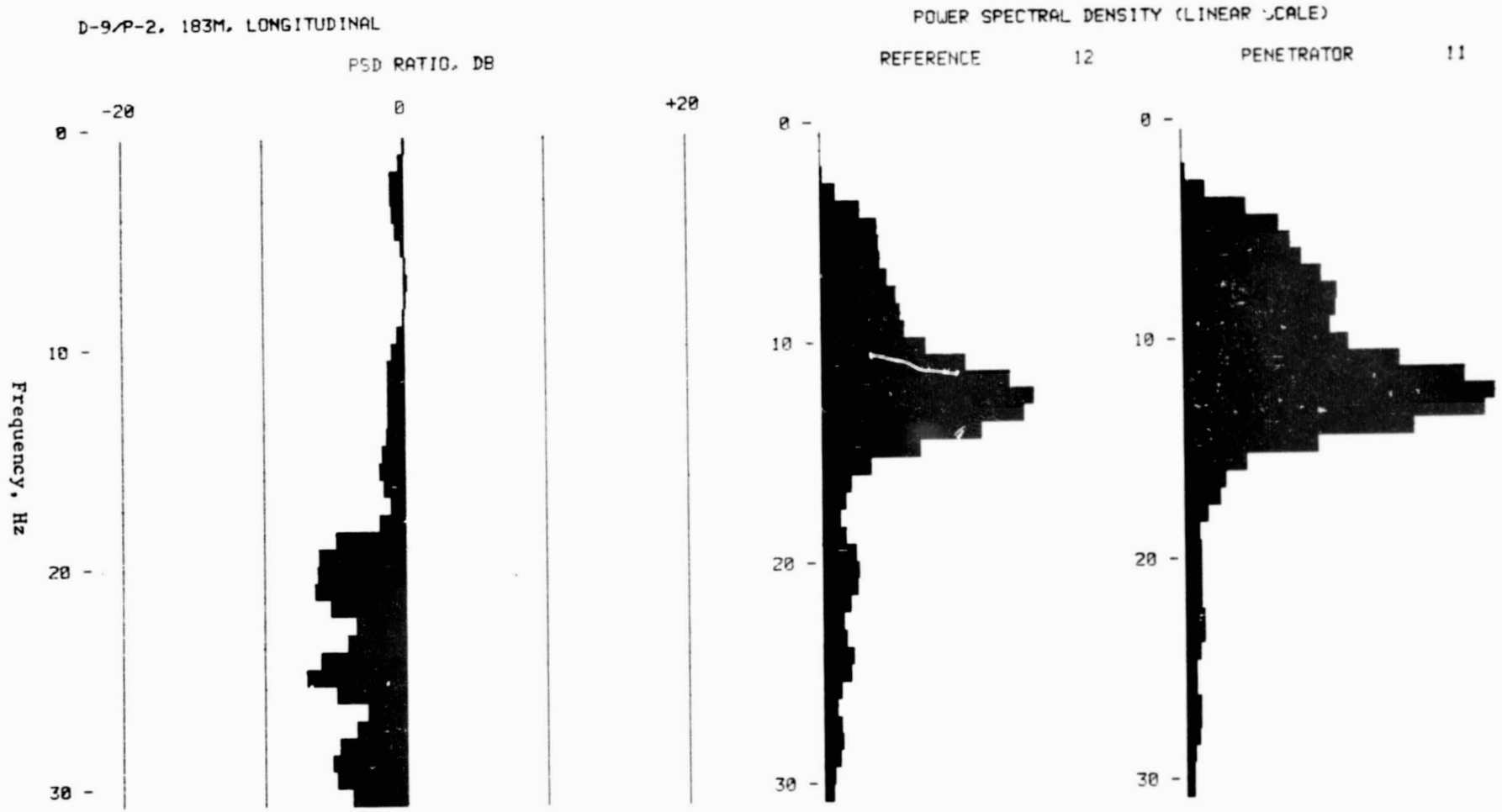

(a) Power spectral densities.

Figure 15.- Longitudinal horizontal power spectral densities, coherence, and cross-phase spectra of seismic signals from a dummy penetrator firing at a distance of 183 m (600 ft), observed by vertical-component geophone at the Tonopah test site, and the penetrator/reference PSD ratio.

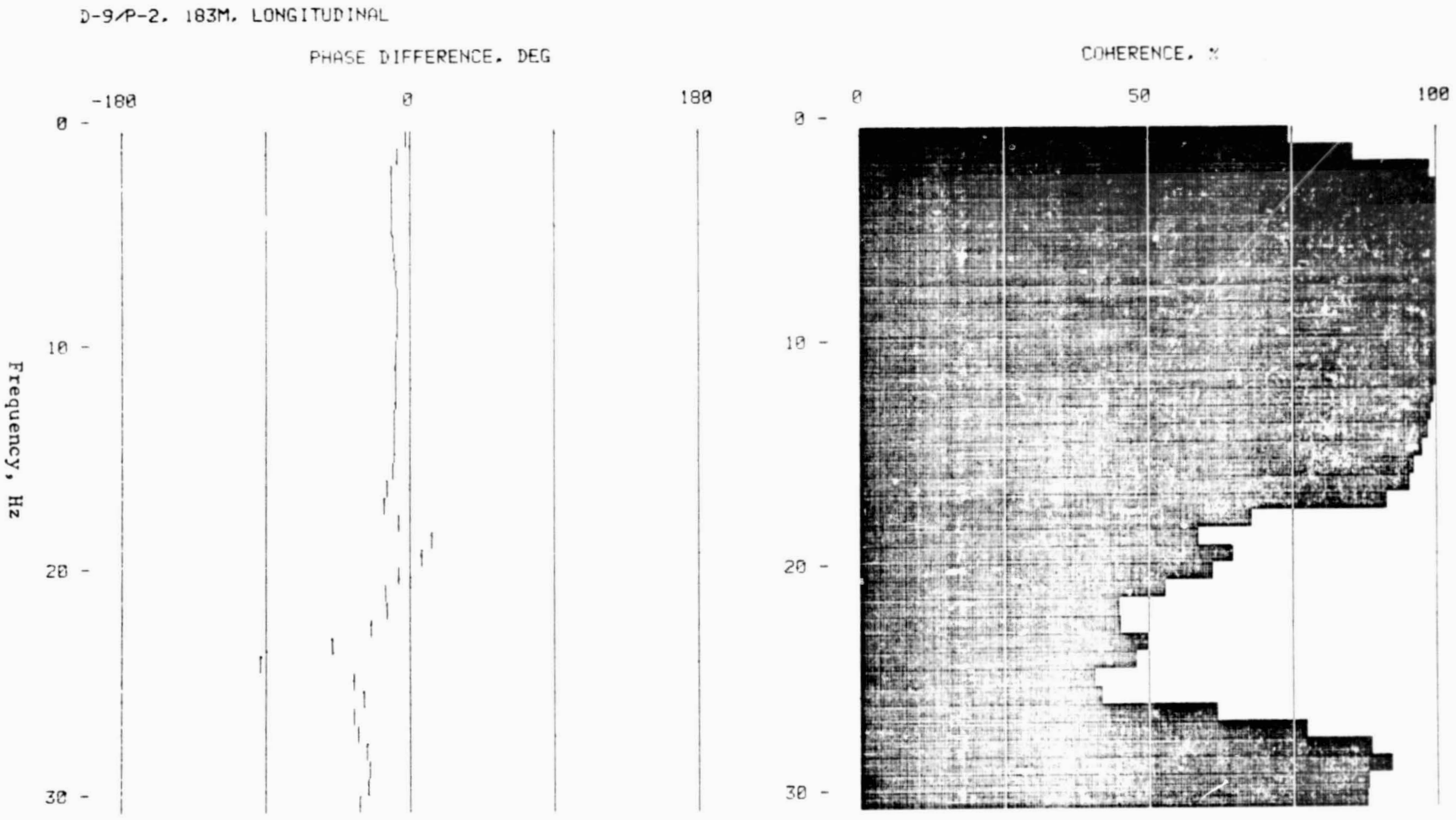

(b) Coherence and cross-phase spectra of the same pair of signals as figure 15(a).

Figure 15.- Concluded.

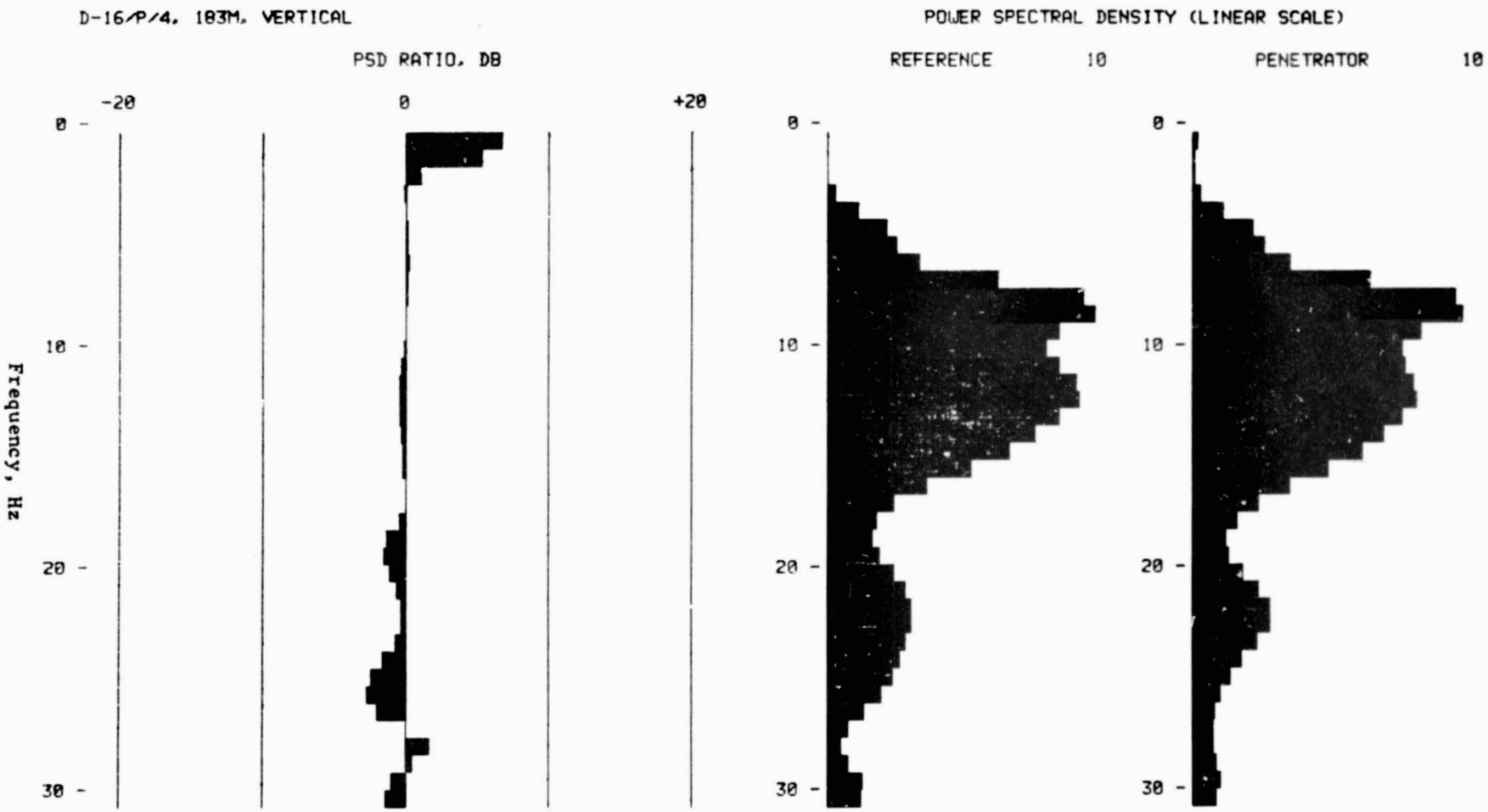

(a) Power spectral densities.

Figure 16.- Vertical power spectral density, coherence, and cross-phase spectra plots of seismic signals from a dummy penetrator firing at a distance of 183 m (600 ft) observed by vertical-component geophones at the White Sands test site, and the penetrator/reference PSD ratio.

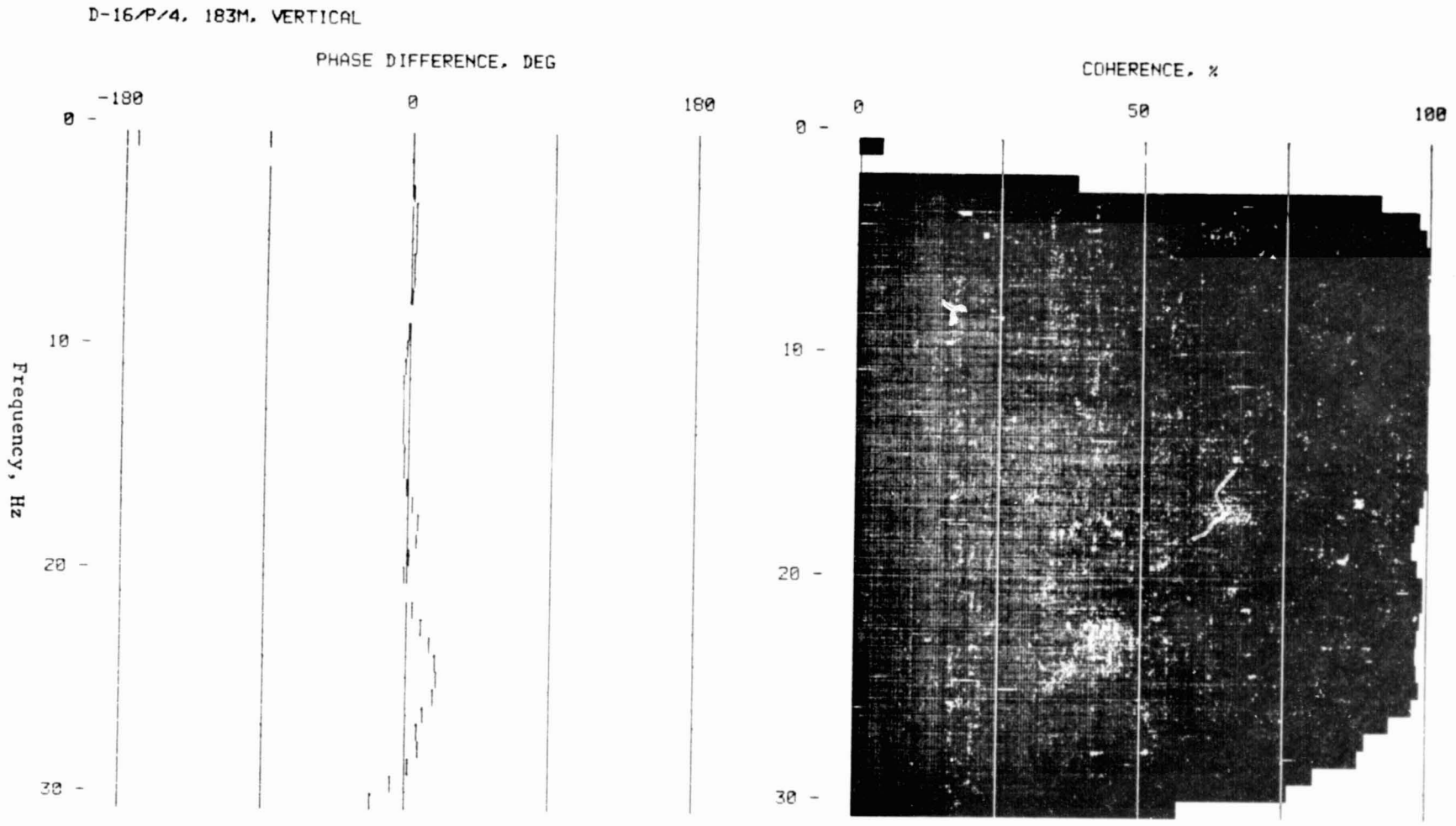

(b) Coherence and cross-phase spectra of the same pair of signals as figure 16(a).

Figure 16.- Concluded.

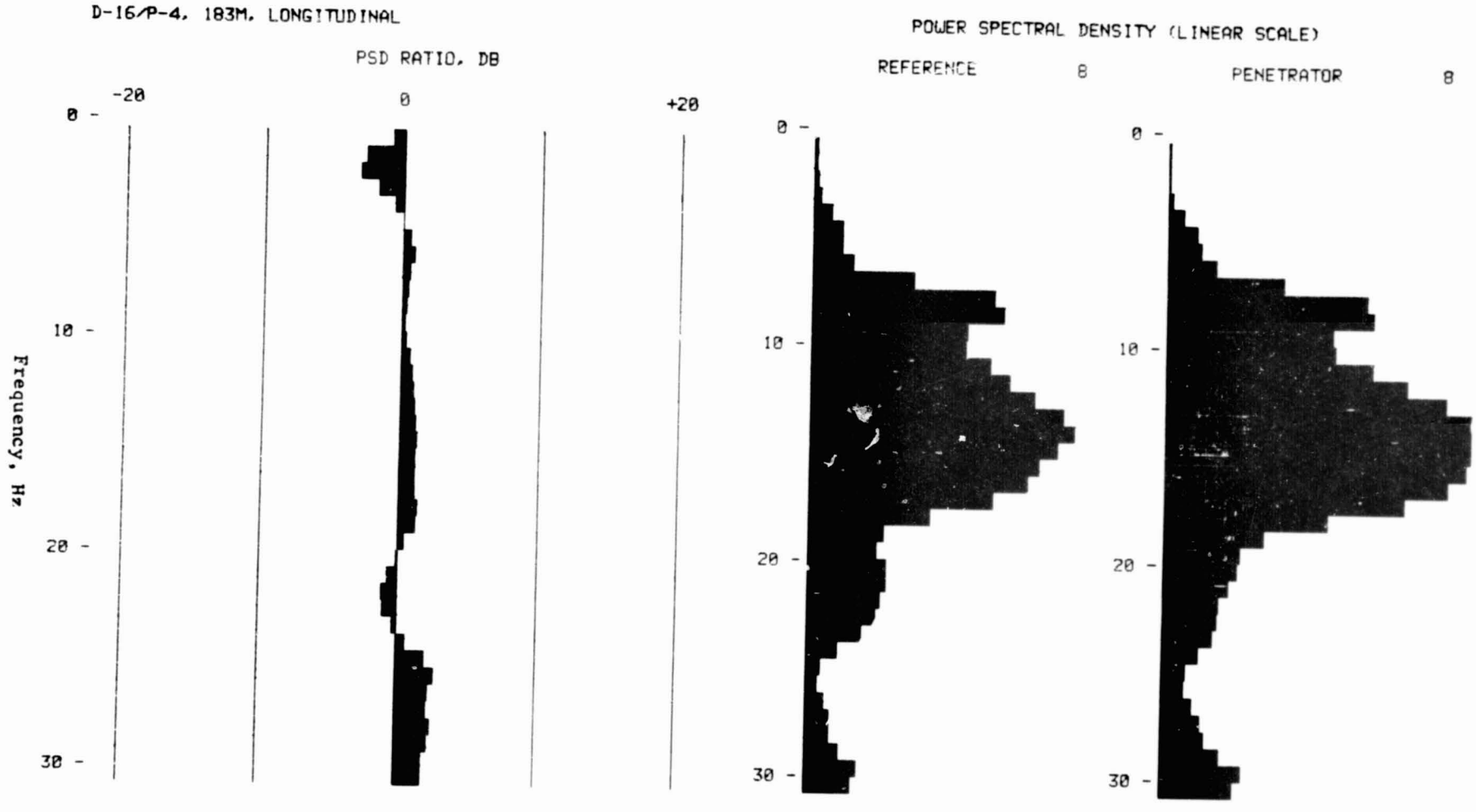

(a) Power spectral densities.

Figure 17.- Longitudinal horizontal power spectral density, coherence, and cross-phase spectra plots of seismic signals from a dummy penetrator firing at a distance of 183 m (600 ft), observed by vertical-component geophones at the White Sands test site, and the penetrator/reference PSD ratio.

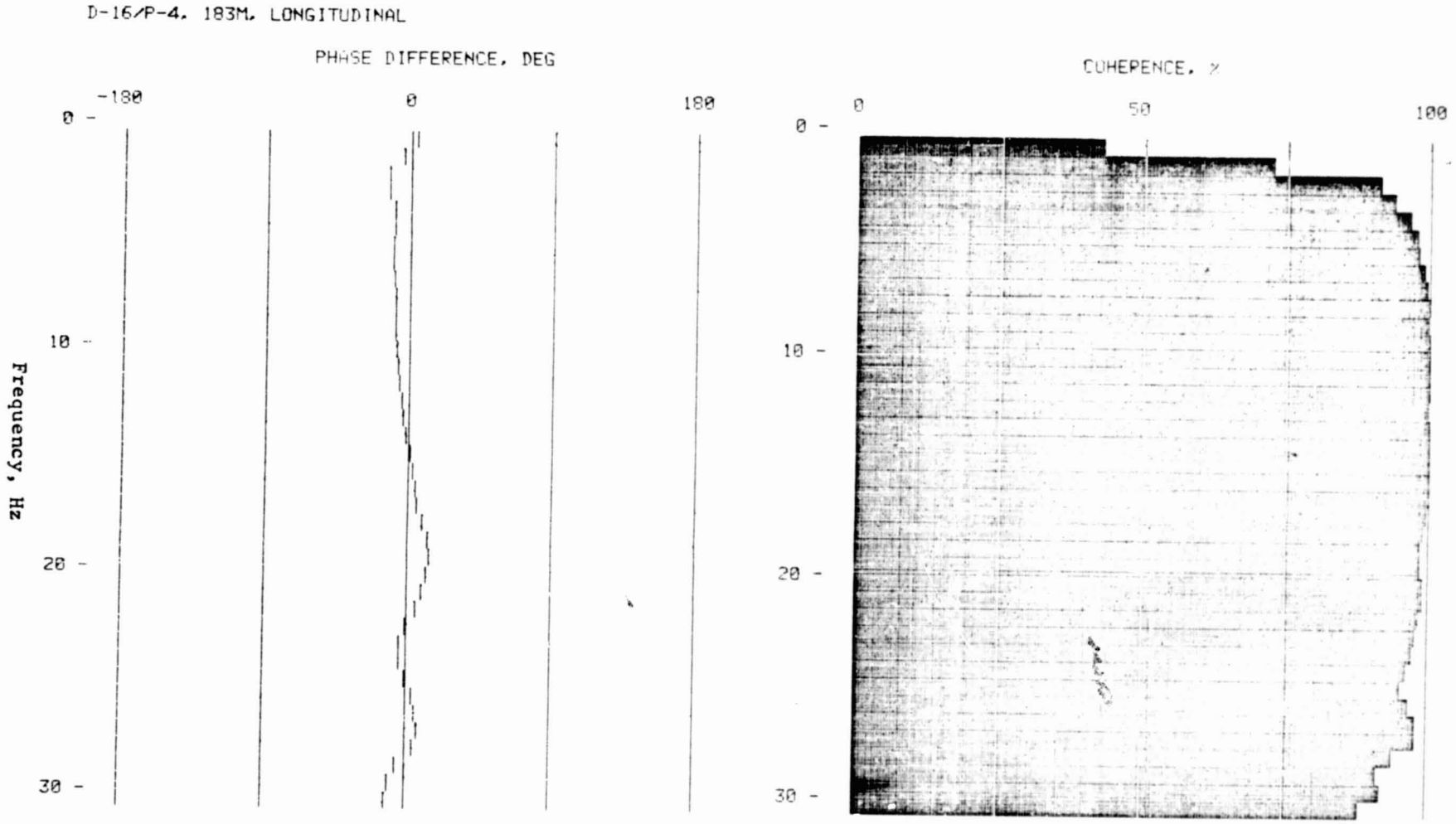

(b) Coherence and cross-phase spectra of the same pair of signals as figure 17(a).

Figure 17.- Concluded.

Extremely low values are always associated with low PSD values and must be discounted. However, a comparison of the penetrator vs reference data for the White Sands tests with the reference vs reference data (Ref./Ref. in table 2) reveals that the lower coherence value is significant only at frequencies above 20 Hz. The coherence spectra thus indicate that the signal waveforms are not significantly affected at either site by using the penetrator for installing the geophone for frequencies below 20 Hz, except for the horizontal component at the Tonopah site, for which one of the penetrators showed a slightly lower coherence.

The phase difference between the penetrator and the reference signals, table 4, generally remains less than 10° for the vertical component at frequencies below 20 Hz. For the horizontal component, it is slightly larger, but the differences generally remain within 20° of each other for the same frequency range. Somewhat larger differences are observed at frequencies above 20 Hz, especially for the horizontal component. As above, extremely large differences are associated with very low PSD values, and must be discounted. The phase spectra thus indicate that phases of the signals are not significantly affected by placing the geophone on the penetrator for frequencies below about 20 Hz. For frequencies between 20 and 30 Hz, some effects are observed — especially for the horizontal component — that appear as a phase lag for the Tonopah site, but as a phase advance for the White Sands site.

The power-spectral density ratio between the penetrator signal and the reference signal, table 2, generally remains well within the uncertainty of instrument sensitivity, estimated to be about ±1 dB, at both sites for frequencies below 10 Hz. (The three vertical component data recordings from the Tonopah site are exceptions, and as discussed earlier, are judged to have been recorded at wrong amplifier gains.) The differences are slightly larger at higher frequencies, but for the vertical component they are no larger than that for the reference/reference value, indicating that they cannot be attributed to the penetrator ground coupling. The difference between the penetrator signal and the reference signal is again slightly larger for the horizontal component than for the vertical component. At frequencies higher than 20 Hz, horizontal signals from the penetrator-mounted geophone are a few decibels lower than the reference at the Tonopah site, and a few decibels higher than the reference at the Tonopah site.

Thus it appears that there is no significant difference in ground coupling between the penetrator-installed geophone and the reference geophone over the range of frequencies of interest in most seismological studies. In the frequency range of 3 to 20 Hz, the penetrator is as firmly coupled to the ground as the reference geophone. In the frequency range of 20 to 30 Hz, the penetrator fired into the dry-lake sediments appear to be slightly less well coupled to the ground than the reference, particularly for horizontal ground vibrations; the penetrator fired into the lava bed appears to be slightly better coupled to the ground than the reference for horizontal ground vibrations. The difference, however, never exceeds 10 dB in this frequency range.

V. DISCUSSION

The results of the analysis described in the preceding section indicate that the penetrator-installed geophones are as well coupled to the ground as the carefully installed reference geophones. This conclusion holds over the frequency range of about 3 Hz to 30 Hz, in which the observed signal strength from dummy-penetrator firings was high enough to allow meaningful comparison. Great care was taken during the present experiments in the emplacement of the reference geophones, using plaster of paris to firmly mount them to specially selected and carefully cleaned sites. Thus it is quite likely that these reference geophones were better coupled to the ground than are some conventionally installed geophones, which might simply be placed on the ground or on an outcrop, or perhaps buried in a shallow hole. Although we make no experimental comparison between the penetrator-mounted geophones and those simply placed on the ground (which appears to be the most likely method of seismometer installation on planetary surfaces from a soft lander at present), it is quite probable that the ground coupling of the former is actually superior to that of the latter.

Small differences were observed between the penetrator-mounted geophones and the reference geophones at the high-frequency end of this range (above 20 Hz). Whether these differences are a consequence of differences in ground coupling or real difference in ground motion at different sites is not known. For frequencies below about 3 Hz, both the level of the source spectrum and the response of the 4.5 Hz geophones were too low to give meaningful data. However, there is no reason to believe that coupling at frequencies below 3 Hz is not as good as that in the 3 to 10 Hz range.

The present experiment was performed using a half-scale model of the penetrator designed for use on Mars; we do not have data to use for extrapolating the present result to full-scale penetrators. A full-scale penetrator would presumably be heavier than a half-scale penetrator, and would also generate a larger disturbed zone around its point of impact. Both of these would contribute to lowering the characteristic frequency of the penetrator/ground system. Although the results of the half-scale test are quite encouraging and although these effects are not likely to alter the results significantly, full-scale tests are needed to evaluate the influence of these factors.

The digitized, three-component, seismic data allow one to try many other signal analyses than those described here. For example, the signals could be enhanced for certain given particle motions and compared. The cross-spectral analysis could be performed separately for different parts of the wave train independently, representing body waves and surface waves. However, after observing the nearly identical waveforms for the penetrator-mounted geophones and the reference geophones, we judged that any further analyses were not necessary.

VI. CONCLUSIONS AND RECOMMENDATIONS

This field experiment demonstrated that seismometers deployed by penetrators will be as well coupled to the ground, for the frequency range of interest in earthquake seismology, as are seismometers installed by the best conventional methods. It is quite likely that they will be better coupled to the ground than would be seismometers simply placed on the ground or buried in a shallow hole. Some differences were observed but only at frequencies higher than those of normal interest to seismology. At these higher frequencies (above 30 Hz), local structural heterogeneities and resonances in the seismometer assembly appear to be more important than the effect due to the possible decoupling of penetrators from the ground.

The use of penetrators as a means of deploying seismometers in remote areas is feasible. For operations at frequencies much higher than those normally of interest in earthquake seismology, possible problems other than decoupling of penetrators from the ground must be considered.

APPENDIX

PENETRATOR AND REFERENCE GEOPHONE CHART RECORDINGS

The following are reduced copies of chart recordings of signals from dummy penetrator (denoted by "D") and artillery gun firings (denoted by "G"). The traces are, from top to bottom, the vertical (V), longitudinal horizontal (L), and transverse horizontal (T) components of the penetrator-mounted geophone signals, and those of the reference geophone signals. The chart sensitivity was fixed at 100 mV/div, giving a full-scale range of ±2.5 V. The distance and the nominal value of amplifier gain are given at the top of each record. The actual overall sensitivites may vary within ±1 dB. Penetrators P-1 and P-2 were fired during the Tonopah (dry-lake bed) test, and P-3 and P-4 were fired during the White Sands (lava flow) test. Refer to table 1 for additional descriptions of each shot.

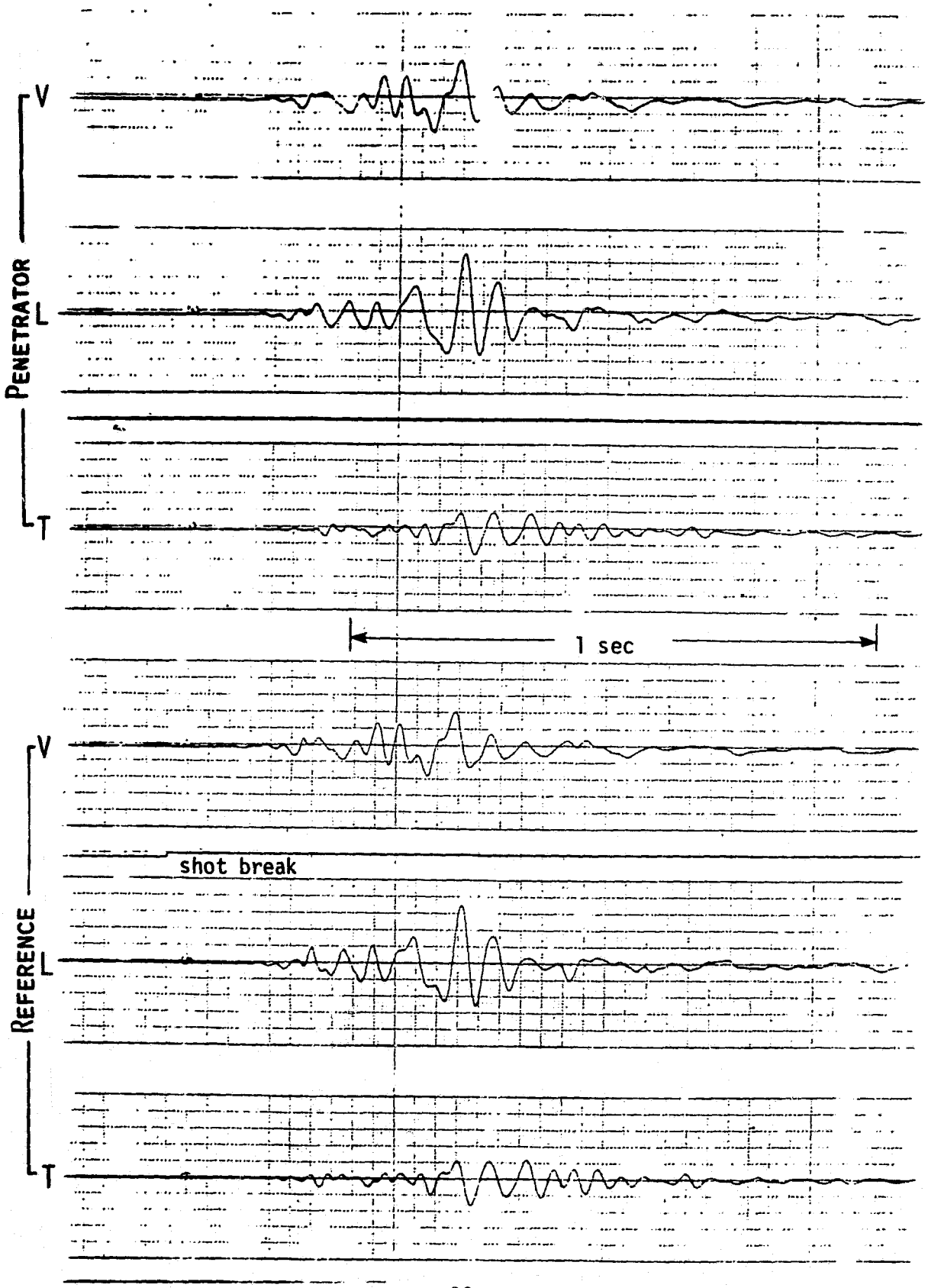
D-1 to P-1, 91 m, 52 dB
V
L
T
PENETRATOR
1 sec
V
shot break
L
T
REFERENCE

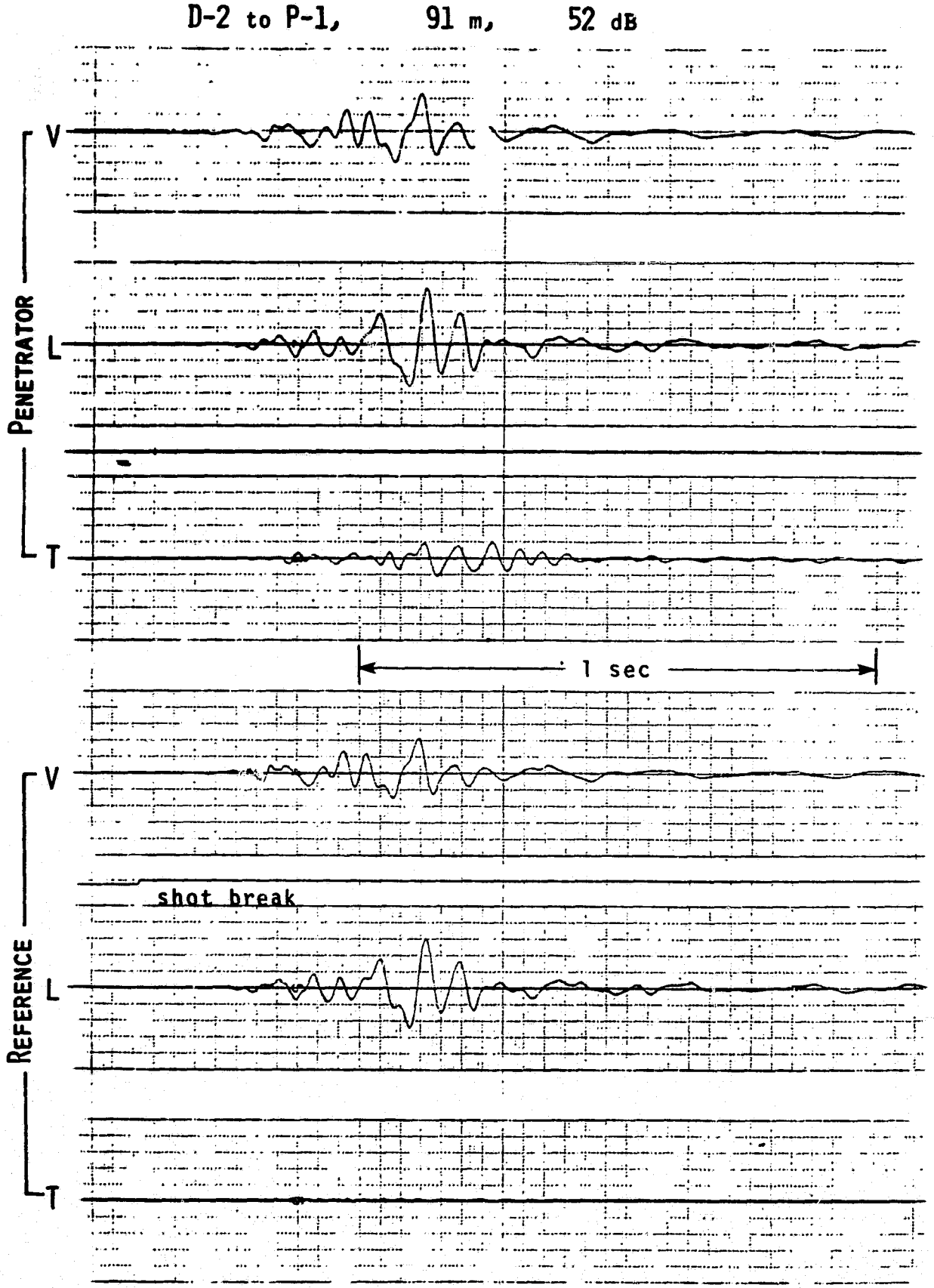
D-2 to P-1, 91 m, 52 dB
PENETRATOR
V
L
T
1 sec
REFERENCE
V
shot break
L
T

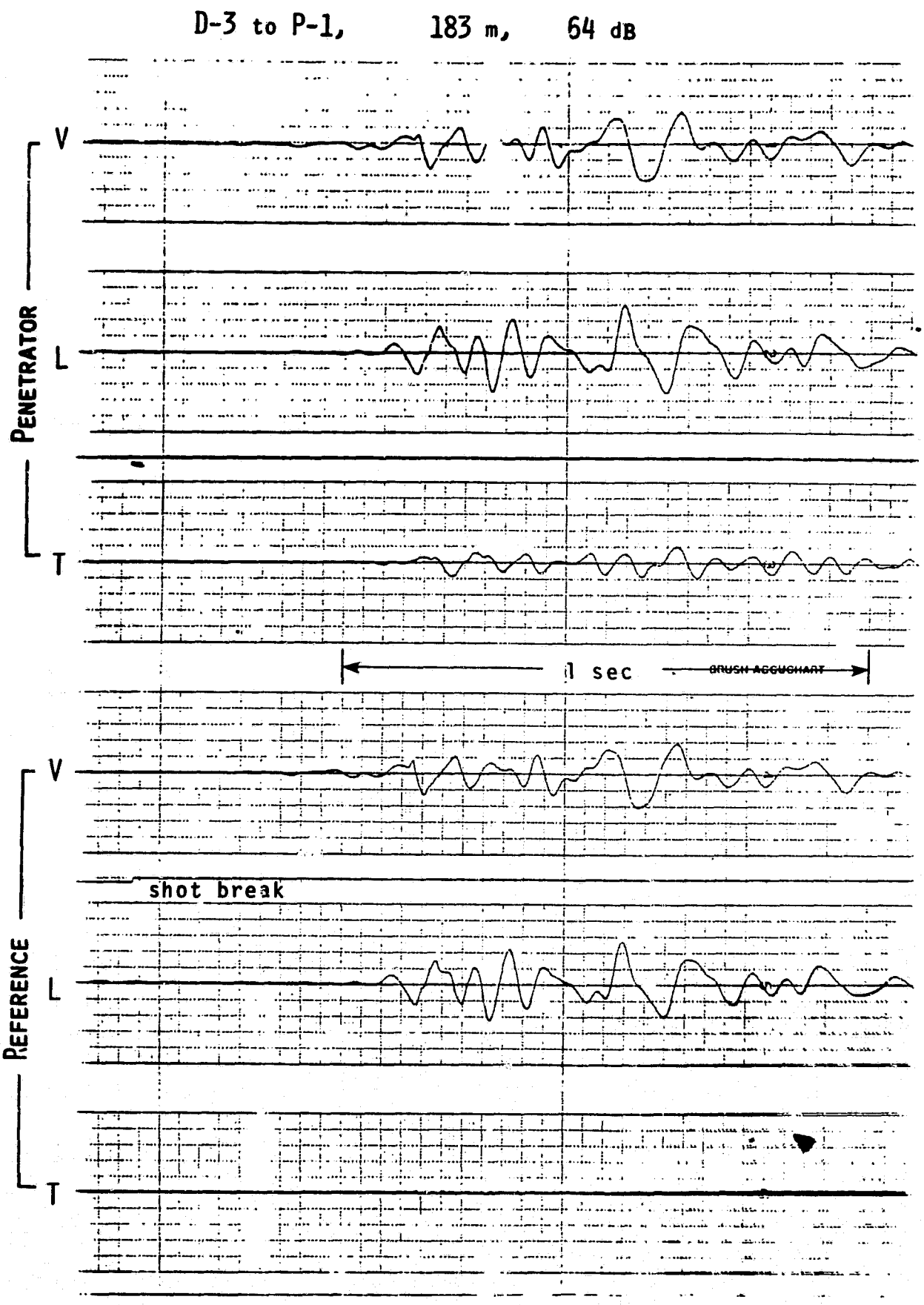
D-3 to P-1, 183 m, 64 dB
PENETRATOR
V
L
T
1 sec
BRUSH ASSOCIATES
REFERENCE
V
shot break
L
T

G-1 to P-2, ~2.5 km, 52 dB

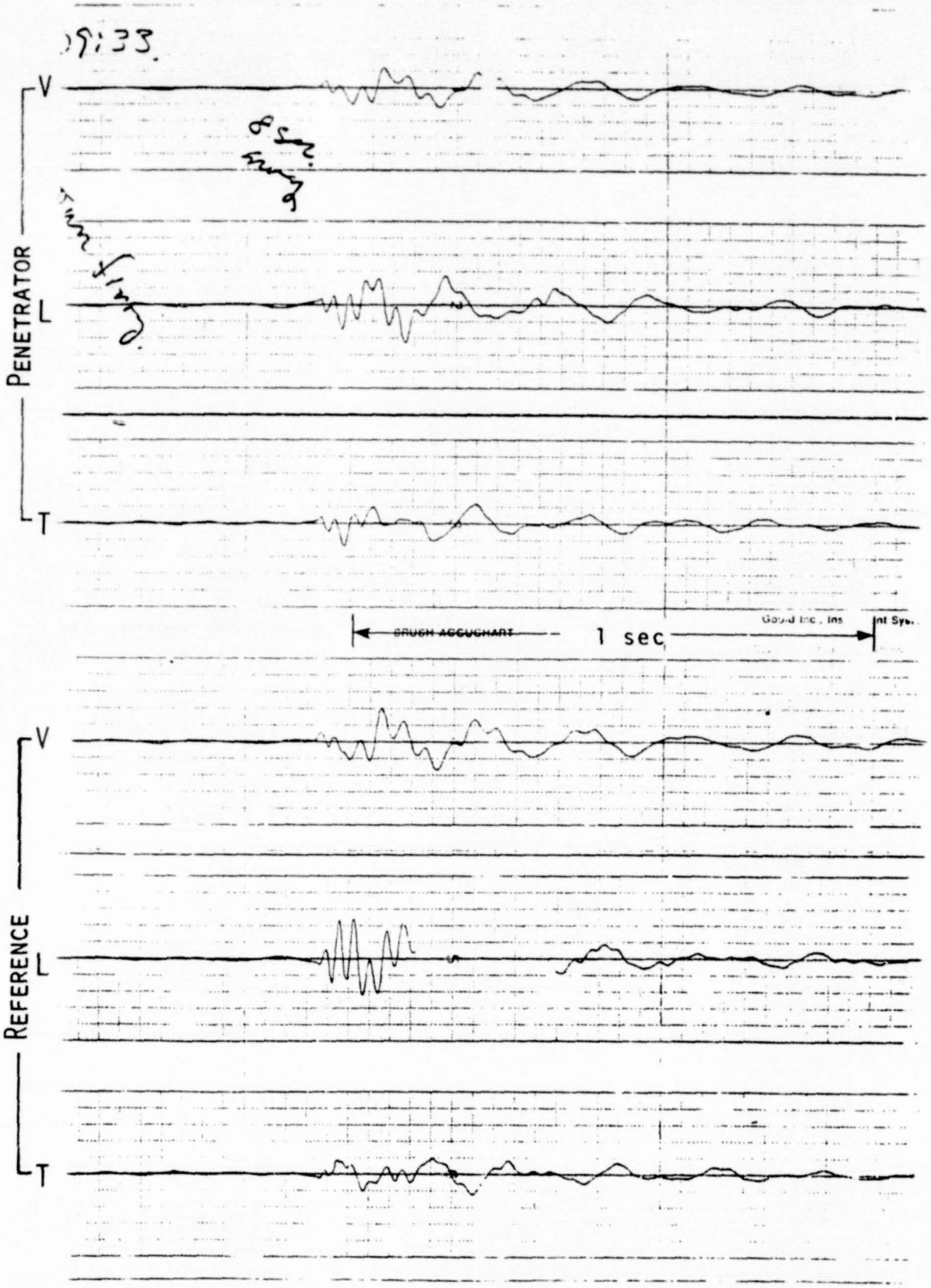

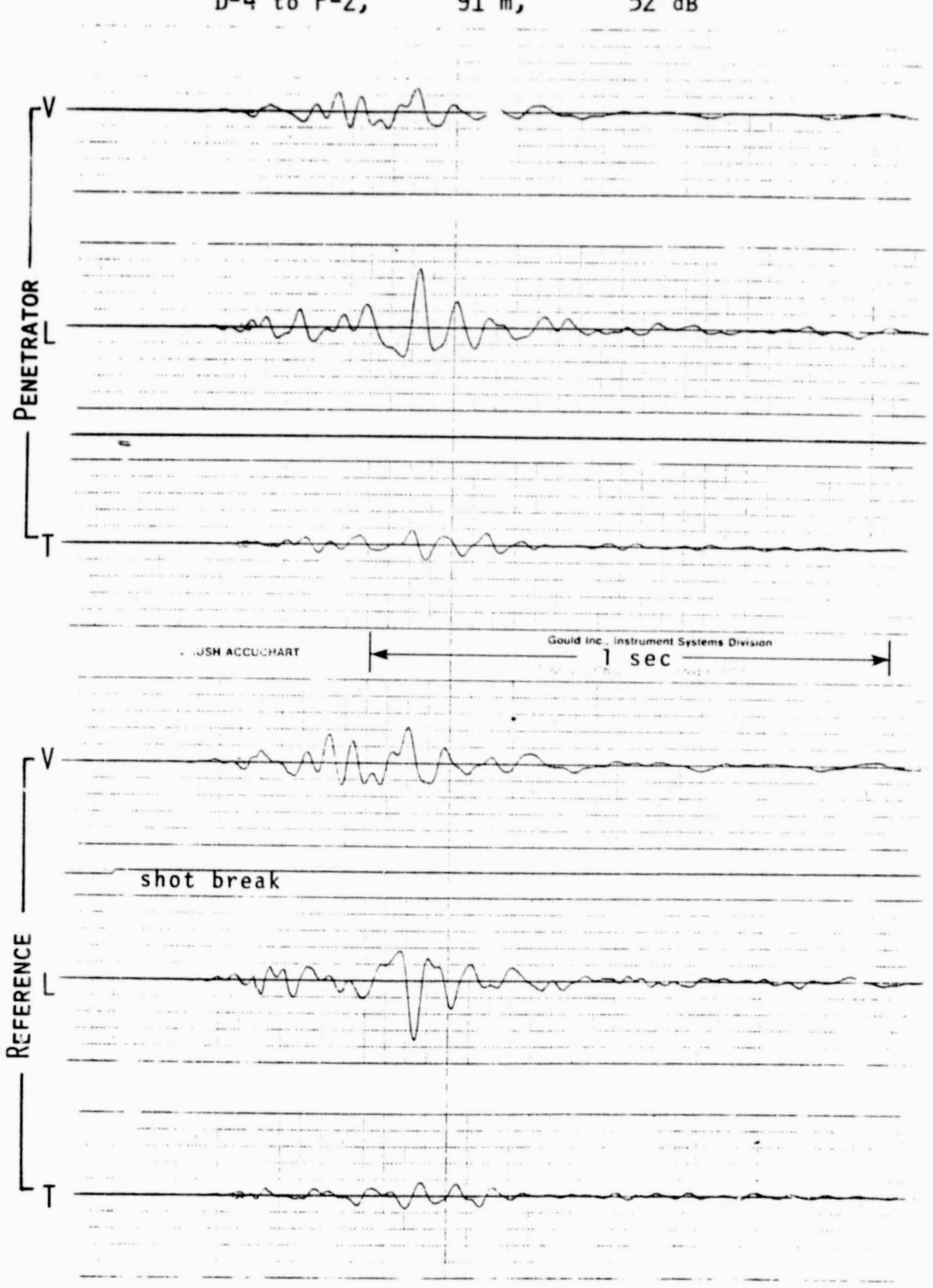
D-4 to P-2, 91 m, 52 dB
V
PENETRATOR
L
T
Gould Inc., Instrument Systems Division
1 sec
V
shot break
REFERENCE
L
T

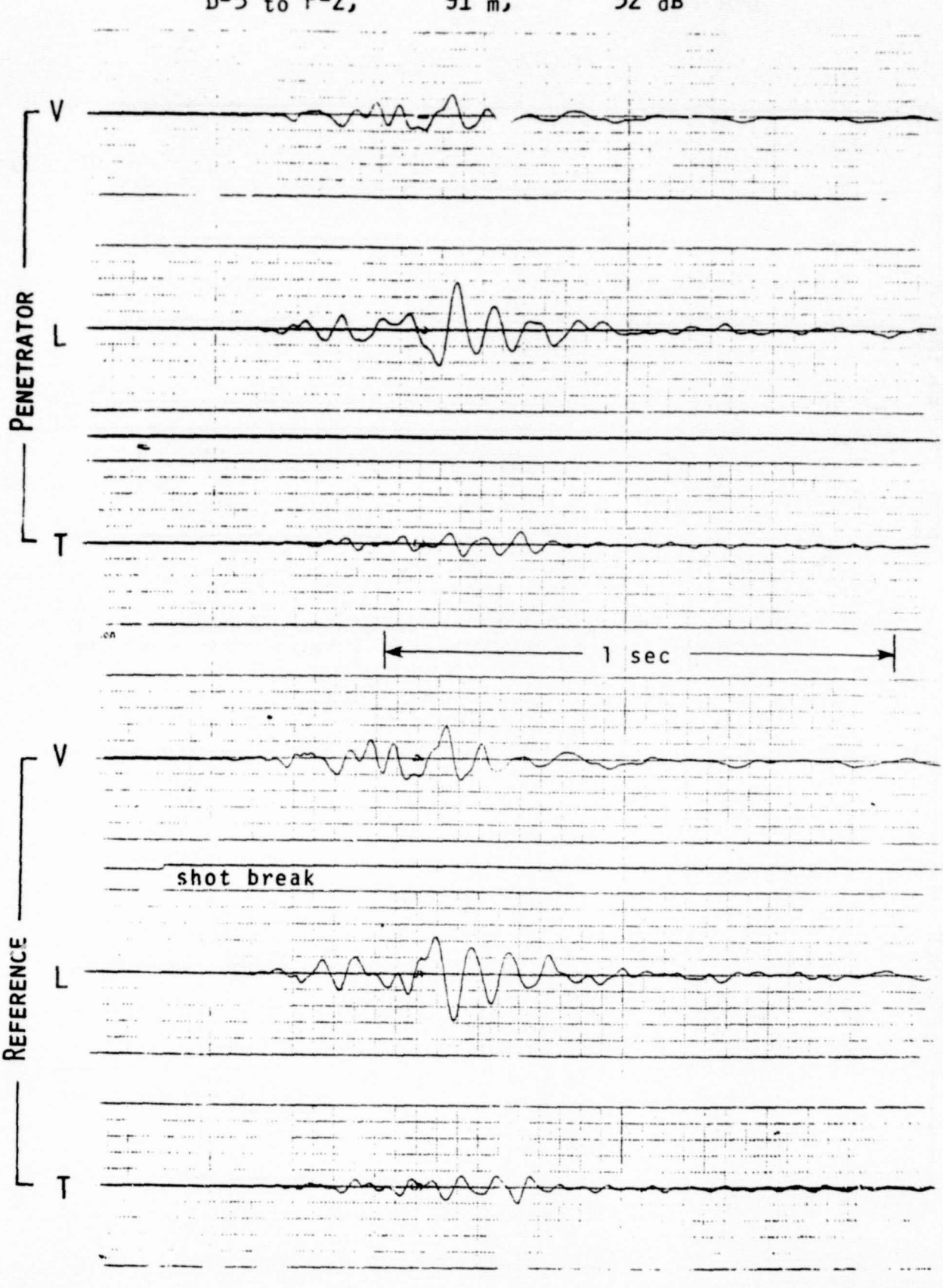
D-5 to P-2, 91 m, 52 dB
PENETRATOR
V
L
T
1 sec
REFERENCE
V
shot break
L
T

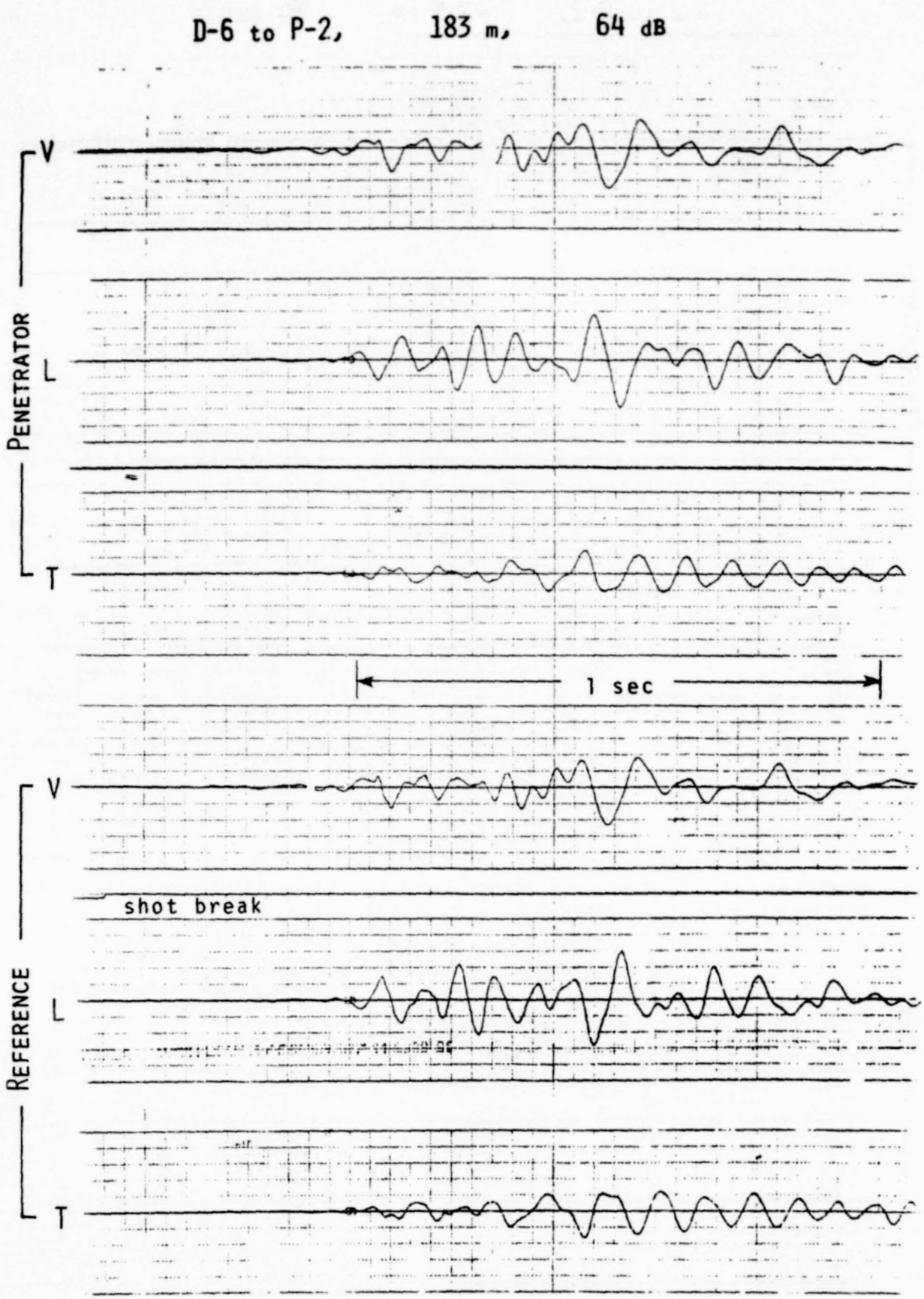
D-6 to P-2, 183 m, 64 dB
PENETRATOR
V
L
T
1 sec
REFERENCE
V
shot break
L
T

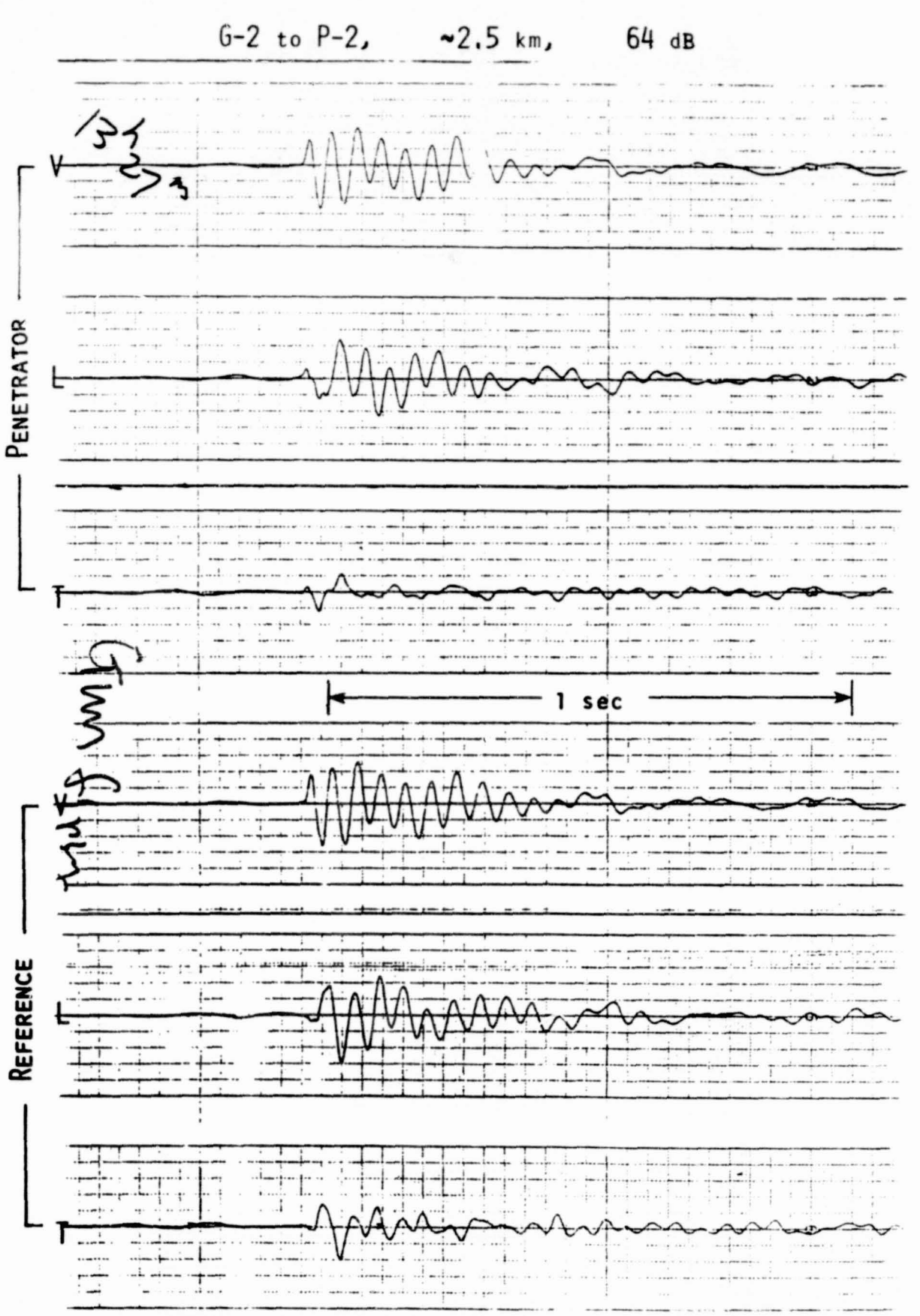
G-2 to P-2, ~2.5 km, 64 dB
PENETRATOR
1 sec
REFERENCE

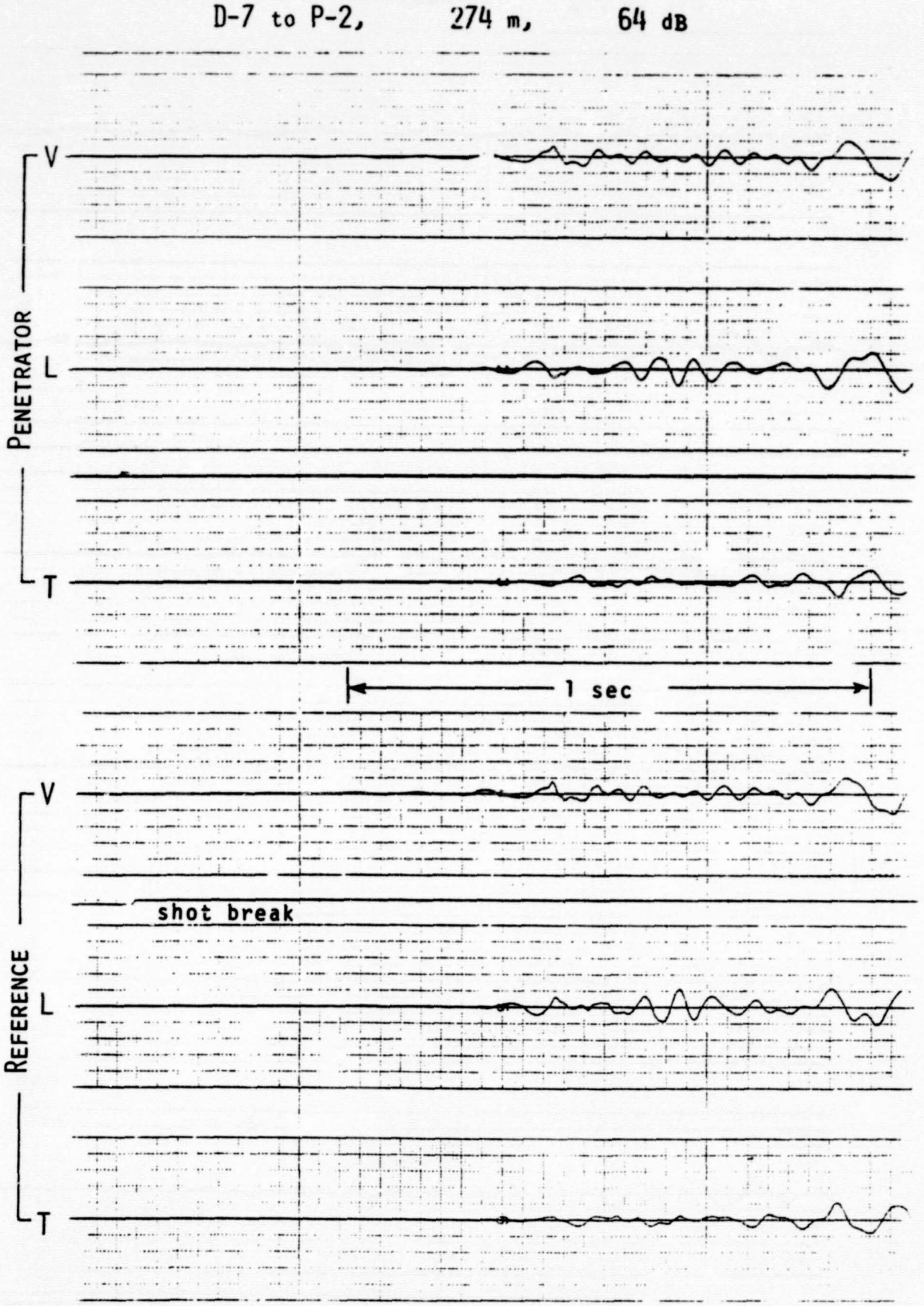
D-7 to P-2, 274 m, 64 dB
PENETRATOR
V
L
T
1 sec
REFERENCE
V
shot break
L
T

D-7 to P-2 continuation

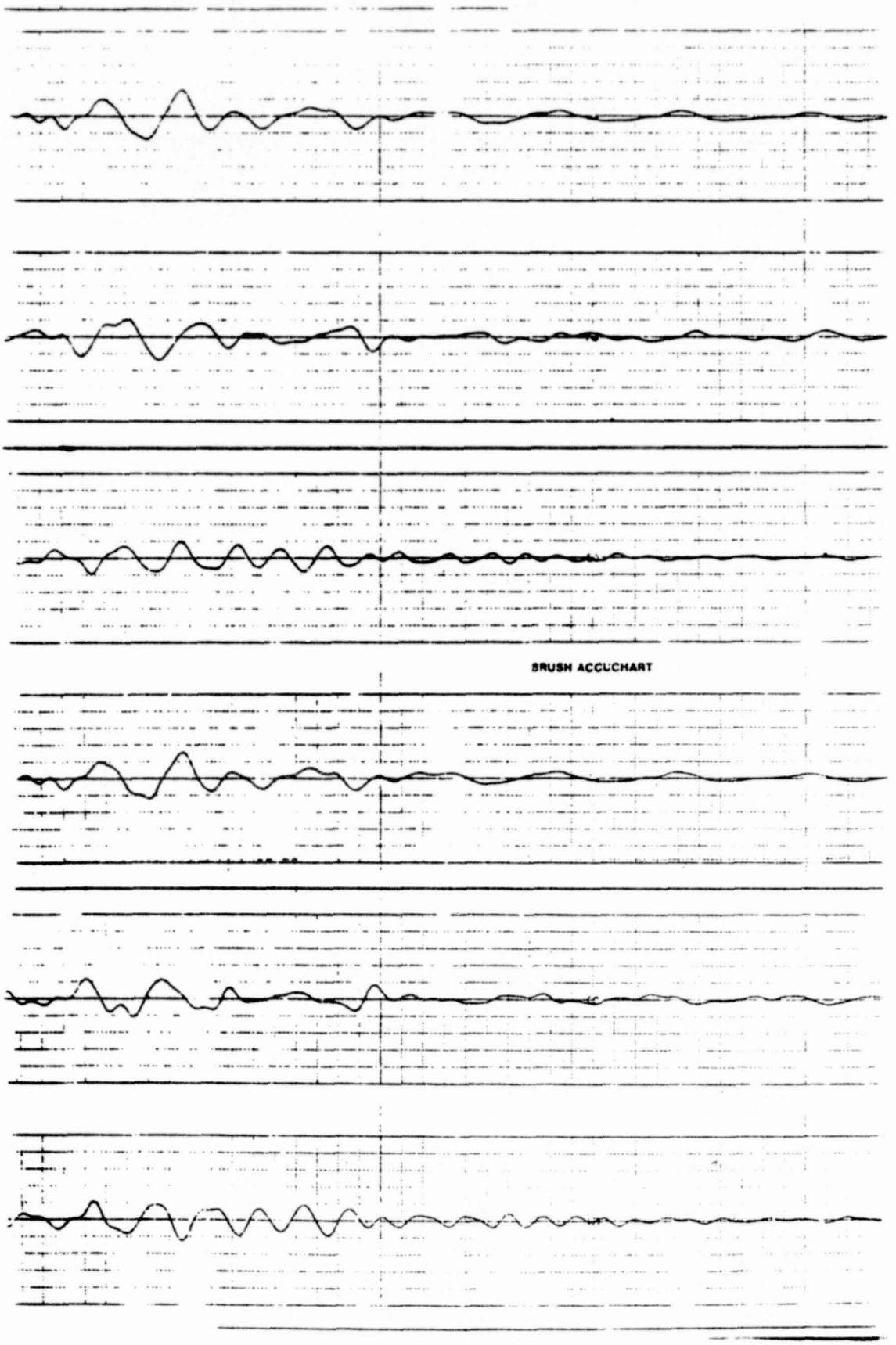

D-9 to P-2, 183 m, 64 dB

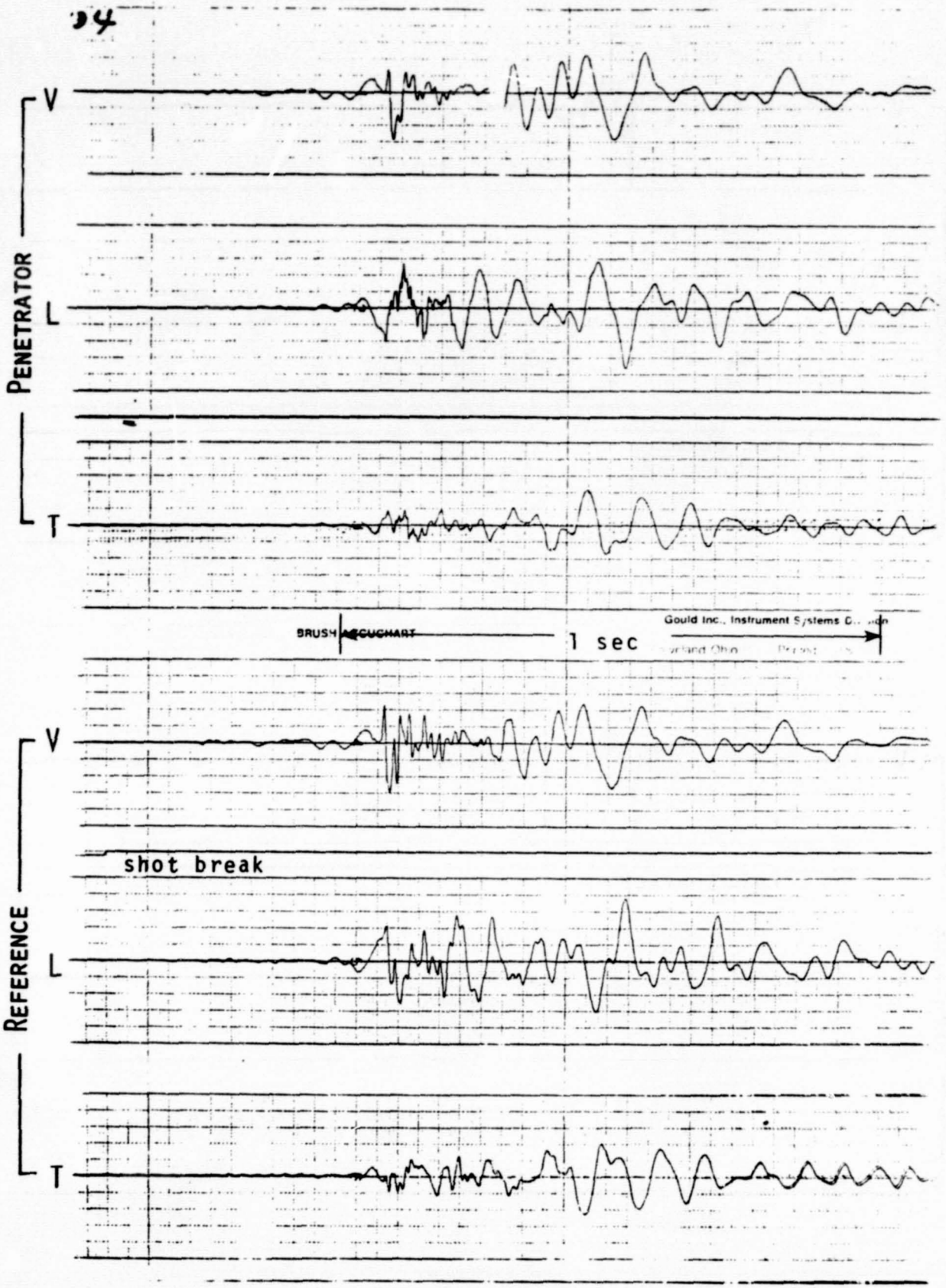

D-10 to REF/REF, 91 m, 58 dB

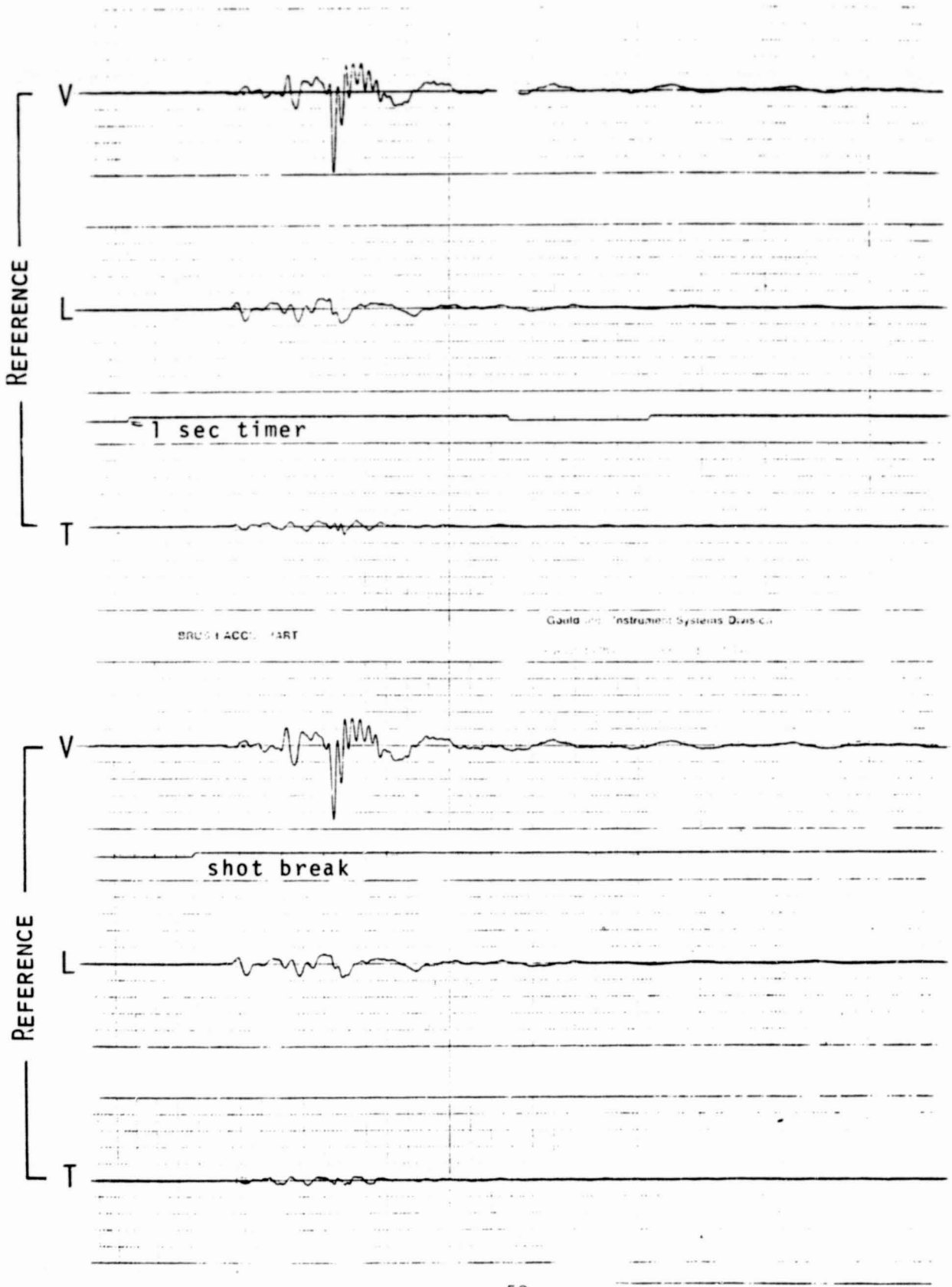

D-11 to P-3, 91 m, 52 dB

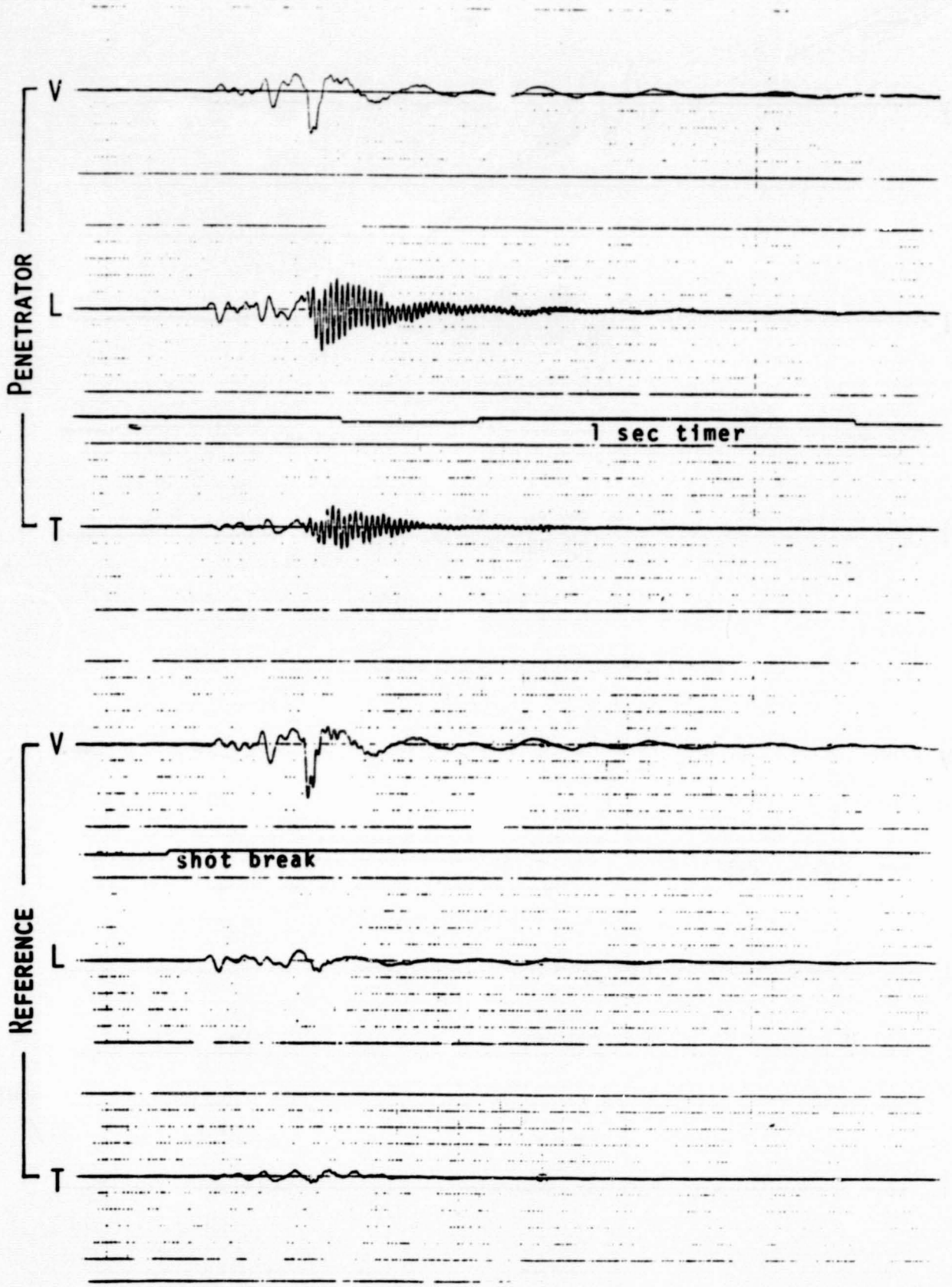

D-12 to P-4, 183 m, 64 dB

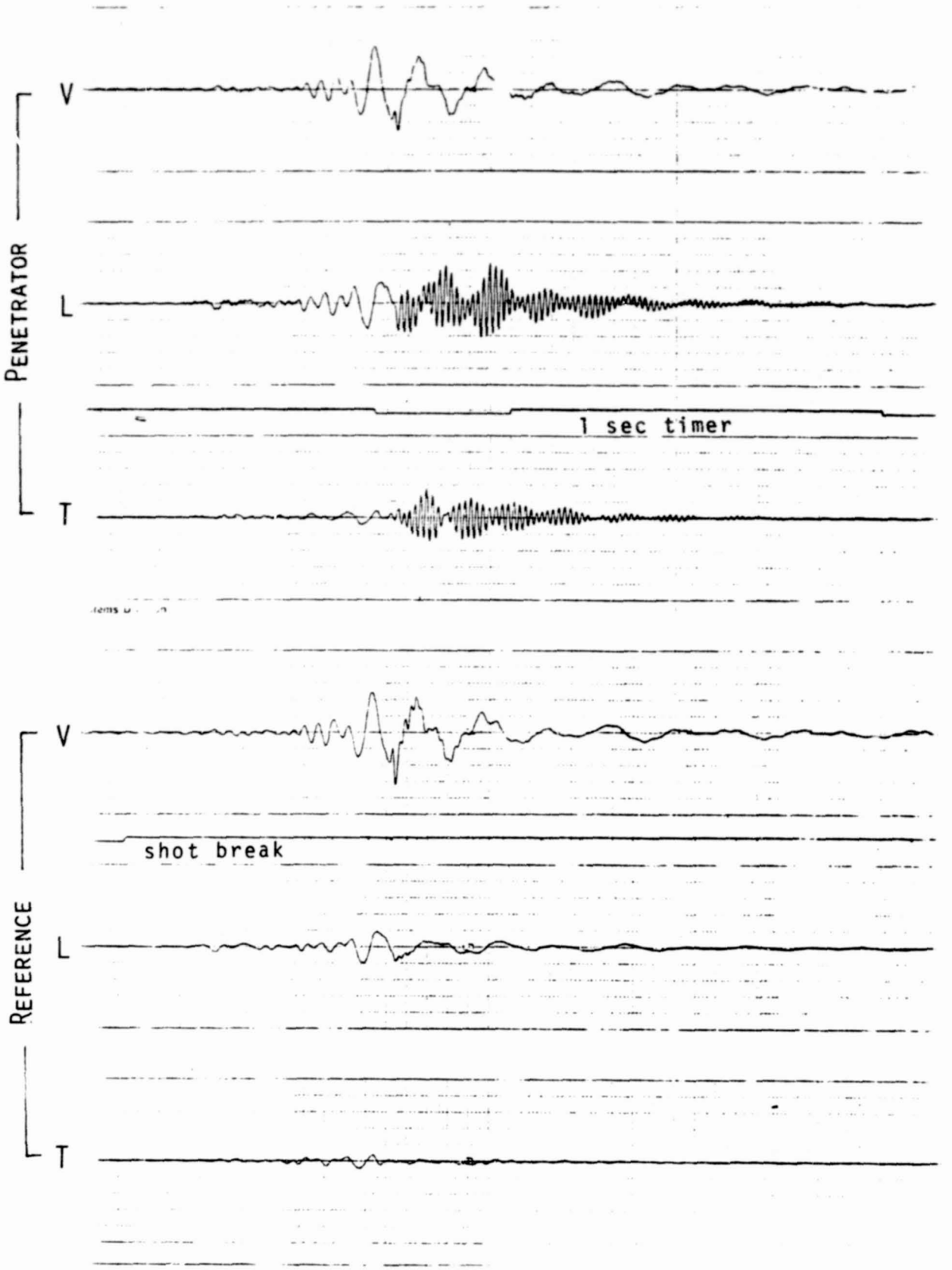

D-15 to P-4, 91 m, 58 dB

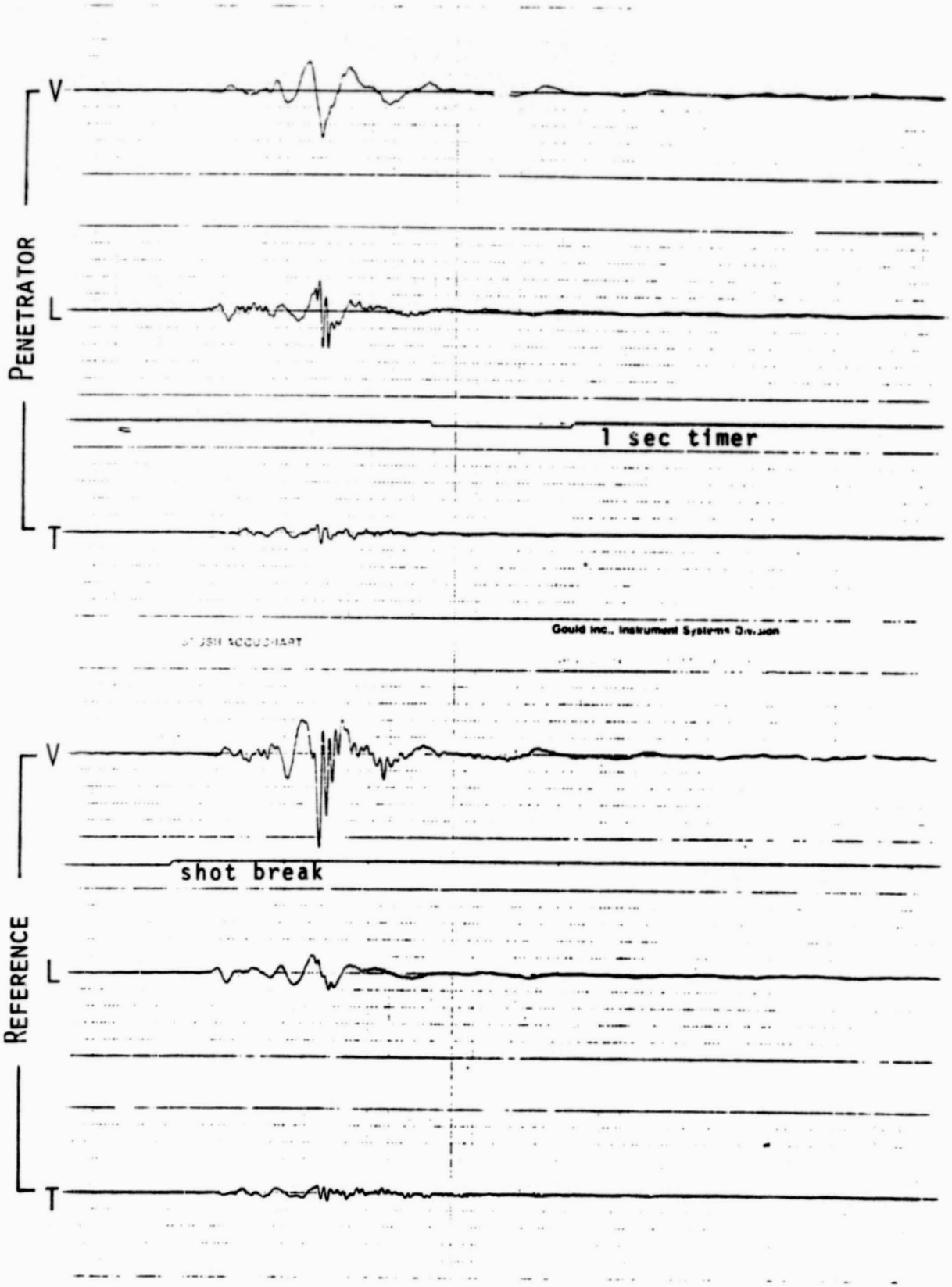

D-16 to P-4, 183 m, 64 dB

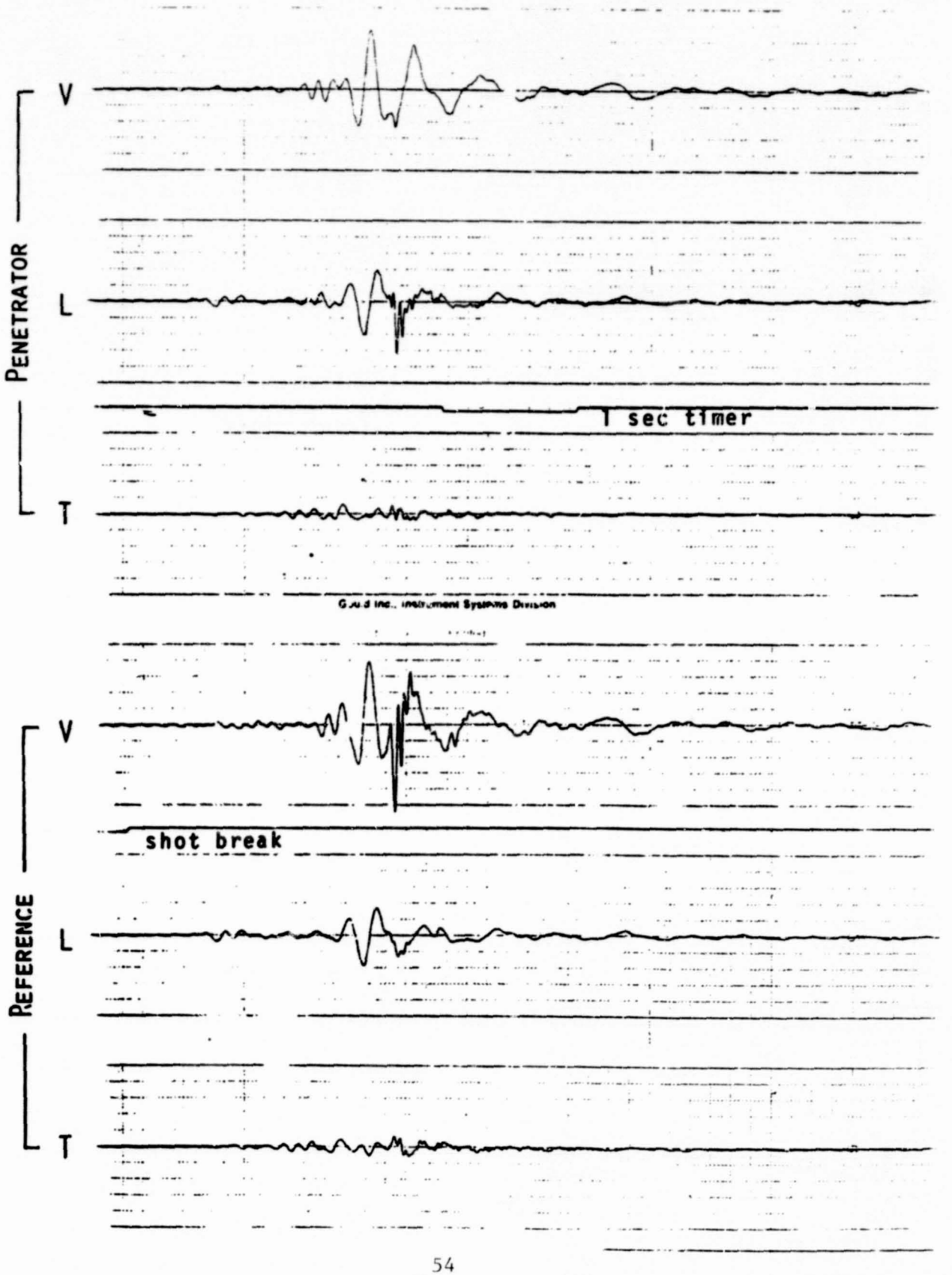

D-17 to P-4, 274 m, 64 dB

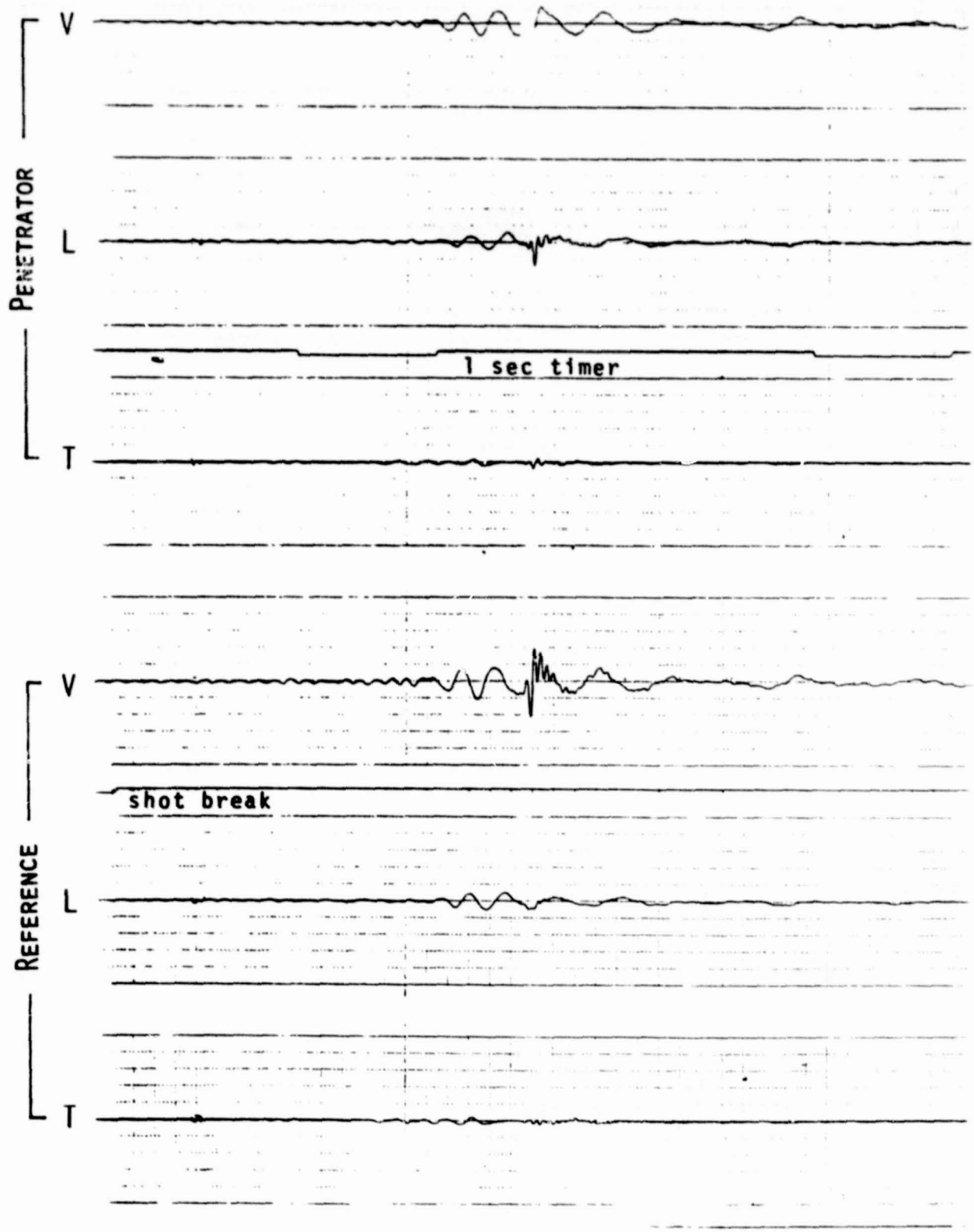

D-18 to P-4, 183 m, 58 dB

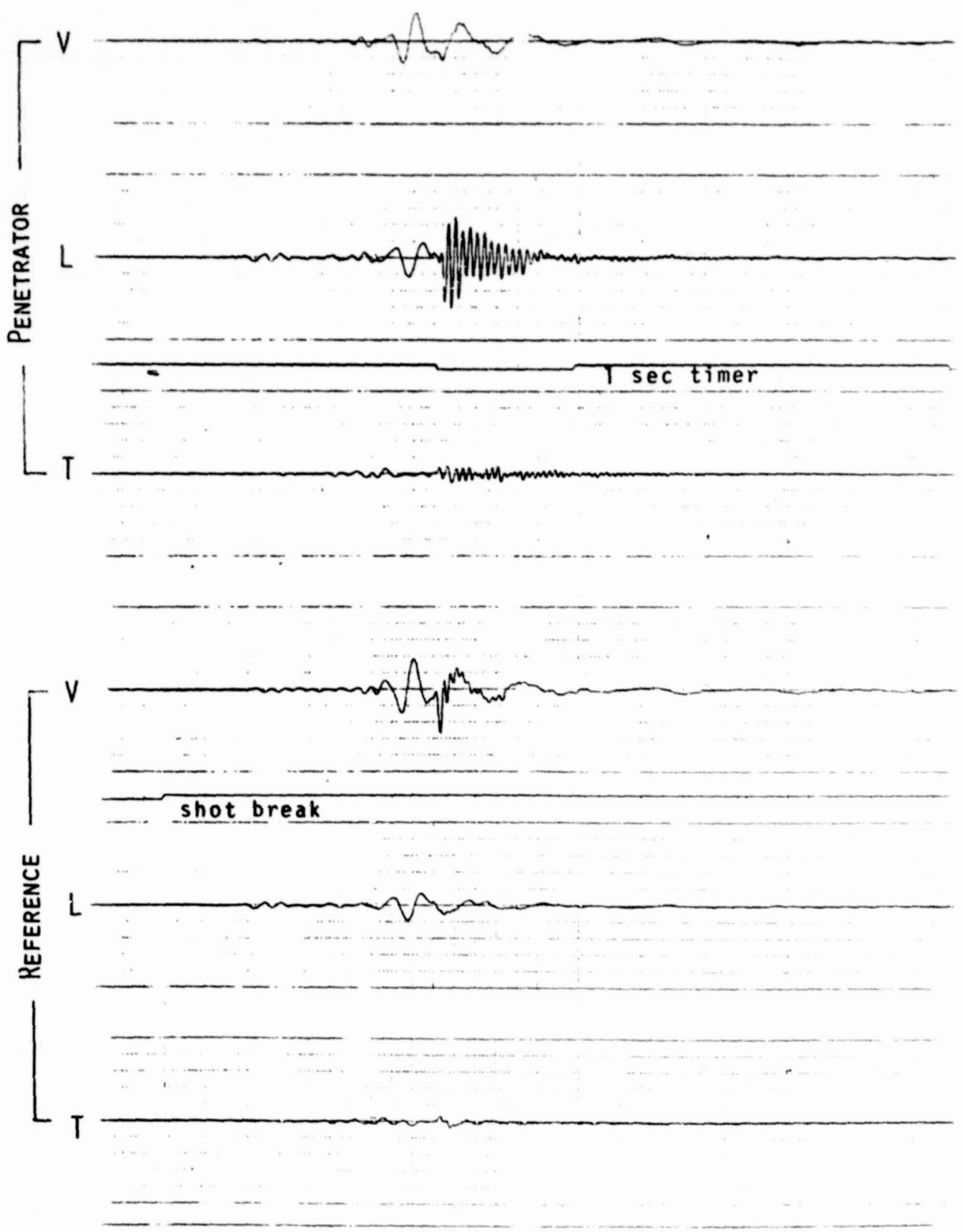

REFERENCES

1. Manning, Larry A., ed.: Mars Surface Penetrator — System Description. NASA TM 73243, Nov. 1977.

2. A Mars 1984 Mission. Mars Science Working Group, NASA TM 78419, July 1977.

3. Report of the Terrestrial Bodies Working Group, Vol. 5 — Mars. Terrestrial Bodies Science Working Group, Jet Propulsion Laboratory Publication 77-51, Sept. 1977.

4. Blanchard, M.; Bunch, T.; Davis, A.; Kyte, F.; Shade, H.; Erlichman, J.; and Polkowski, G.: Results of Analyses Performed on Soil Adjacent to Penetrators Emplaced into Sediments at McCook, Nebraska, Jan. 1976. NASA TN D-8500, July 1977.

5. Blanchard, M.; Bunch, T.; Davis, A.; Shade, H.; Erlichman, J.; and Polkowski, G.: Results of Analyses Performed on Basalt Adjacent to Penetrators Emplaced into Volcanic Rock at Amboy, California, April 1976. NASA TP-1026, Sept. 1977.

6. Marine Sediment Penetrator Instrument Coupling. Prepared by Woodward-Clyde Consultants, for Sandia Laboratories, San Francisco, Calif., Jan. 1977.

7. Kanasewich, E. R.: Time Sequence Analysis in Geophysics. University of Alberta Press, Edmonton, 1973.